Spc98p Directs the Yeast γ-Tubulin Complex into the Nucleus and Is Subject to Cell Cycle-dependent Phosphorylation on the Nuclear Side of the Spindle Pole Body

Gislene Pereira,* Michael Knop,* and Elmar Schiebel*†

Max-Planck Institut für Biochemie, 82152 Martinsried, Germany

In the yeast *Saccharomyces cerevisiae*, microtubules are organized by the spindle pole body (SPB), which is embedded in the nuclear envelope. Microtubule organization requires the γ-tubulin complex containing the γ-tubulin Tub4p, Spc98p, and Spc97p. The Tub4p complex is associated with cytoplasmic and nuclear substructures of the SPB, which organize the cytoplasmic and nuclear microtubules. Here we present evidence that the Tub4p complex assembles in the cytoplasm and then either binds to the cytoplasmic side of the SPB or is imported into the nucleus followed by binding to the nuclear side of the SPB. Nuclear import of the Tub4p complex is mediated by the essential nuclear localization sequence of Spc98p. Our studies also indicate that Spc98p in the Tub4p complex is phosphorylated at the nuclear, but not at the cytoplasmic, side of the SPB. This phosphorylation is cell cycle dependent and occurs after SPB duplication and nucleation of microtubules by the new SPB and therefore may have a role in mitotic spindle function. In addition, activation of the mitotic checkpoint stimulates Spc98p phosphorylation. The kinase Mps1p, which functions in SPB duplication and mitotic checkpoint control, seems to be involved in Spc98p phosphorylation. Our results also suggest that the nuclear and cytoplasmic Tub4p complexes are regulated differently.

INTRODUCTION

Tubulin is a heterodimer composed of α- and β-tubulin that assembles into hollow cylinders known as microtubules. Microtubule formation can be divided into a nucleation and a polymerization step. During nucleation, tubulin monomers assemble to form oligomeric structures that eventually form a closed cylinder. Tubulin molecules then polymerize at the ends of the microtubule cylinder, resulting in its elongation (reviewed by Mandelkow and Mandelkow, 1993). In many eukaryotic cells, microtubule nucleation takes place at morphologically distinct structures known as basal bodies, centrosomes, nucleus-associated bodies, or spindle pole bodies (SPB) (reviewed by Kellogg *et al.*, 1994; Pereira and Schiebel, 1997). To collectively define such microtubule nucleation activities, Picket-Heaps (1969) coined the generic term microtubule-organizing center.

The discovery of γ-tubulin as an universal component of microtubule-organizing centers that is involved in microtubule nucleation supports the idea that microtubule assembly is conserved on the molecular level (Weil *et al.*, 1986; Oakley and Oakley, 1989; Oakley *et al.*, 1990; Oakley, 1992; Horio *et al.*, 1991; Stearns *et al.*, 1991; Zheng *et al.*, 1991; Lopez *et al.*, 1995; Sobel and Snyder, 1995; Akashi *et al.*, 1997). Additional studies have shown that γ-tubulin is in a complex with other proteins (Stearns and Kirschner, 1994; Zheng *et al.*, 1995; Moudjou *et al.*, 1996). For example, γ-tubulin is present in a large 25S complex in the cytoplasm of frog eggs and somatic cells (Stearns and Kirschner, 1994; Zheng *et al.*, 1995; Moudjou *et al.*, 1996). Purification of this complex from mitotic frog eggs revealed

---

* Present address: The Beatson Institute for Cancer Research, Garscube Estate, Switchback Road, Bearsden, Glasgow G61 1 BD, United Kingdom.
† Corresponding author.

at least seven proteins including α-, β- and γ-tubulin and additional proteins with apparent molecular weights of 75, 109, 133, and 195 kDa (Zheng *et al.*, 1995).

The SPB of *Saccharomyces cerevisiae* is a multilayered structure that is embedded in the nuclear envelope (see Figure 11). Functions for some of its substructures have been deduced by electron microscopy. The outer and inner plaques organize the cytoplasmic and nuclear microtubules, respectively. The central plaque is involved in the embedding of the SPB into the nuclear envelope (Byers and Goetsch, 1975; Byers, 1981). It is important to note that the nuclear envelope remains intact during the entire cell cycle of a yeast cell. This has the consequence that the inner plaque is always localized in the nucleus, while the outer plaque is directed toward the cytoplasm.

The γ-tubulin of yeast *S. cerevisiae*, named Tub4p, forms a stable complex of approximately 6S with the SPB components Spc98p and Spc97p that is named the Tub4p complex (Geissler *et al.*, 1996; Knop *et al.*, 1997; Knop and Schiebel, 1997). Interestingly, homologs of Spc98p exist in human, *Xenopus laevis* and *Drosophila* γ-tubulin complexes (Murphy and Stearns, personal communication; Zheng, personal communication). The purification of the Tub4p complex revealed that it contains two or more molecules of Tub4p, one of Spc98p, and one of Spc97p (Knop *et al.*, 1997; Knop and Schiebel, 1997). The components of the Tub4p complex have been localized to the outer and inner plaques of the SPB, the substructures that organize the nuclear and cytoplasmic microtubules, respectively (Rout and Kilmartin, 1990; Spang *et al.*, 1996a; Knop *et al.*, 1997). Phenotypic analysis of temperature-sensitive alleles of *TUB4*, *SPC98*, and *SPC97* point to a function of the complex in formation and organization of the mitotic spindle (Geissler *et al.*, 1996; Spang *et al.*, 1996a; Knop *et al.*, 1997) as well as microtubule nucleation by the new SPB (Marschall *et al.*, 1996). *SPC97* is also required for SPB duplication (Knop *et al.*, 1997).

The localization of the Tub4p complex at the nuclear and cytoplasmic side of the SPB raises questions about the assembly and nuclear transport of the Tub4p complex. In addition, the assembled Tub4p complex has to interact with other SPB components. Recently, we have shown that Spc98p and Spc97p of the Tub4p complex bind to the amino-terminal domain of Spc110p (Knop and Schiebel, 1997), a filamentous protein that connects the central plaque with the inner plaque (Rout and Kilmartin, 1990; Kilmartin *et al.*, 1993; Kilmartin and Goh, 1996). Since the amino-terminal domain of Spc110p is only located toward the inner plaque (Spang *et al.*, 1996b), a protein other than Spc110p must function as a docking site for the Tub4p complex at the outer plaque. Whether the Tub4p complex is differently regulated at its two locations, e.g., by modification, is another important question.

In this paper we investigated biosynthetic as well as regulative aspects of the γ-tubulin complex of *S. cerevisiae*. We present evidence that the Tub4p complex is assembled in the cytoplasm and that it is transported into the nucleus via an essential nuclear localization sequence (NLS) in Spc98p. The Tub4p complex is then anchored to the inner plaque via the amino-terminal domain of Spc110p. Spc98p is phosphorylated at the inner plaque of the SPB in a cell cycle-dependent manner, while Spc98p at the outer plaque seems not to be subject to such a modification.

MATERIALS AND METHODS

Growth Conditions and Yeast Strains

Yeast cells were grown in yeast extract, peptone, and dextrose growth medium (YPD). Synthetic complete medium (SC) was prepared as described with either glucose or raffinose and galactose as carbon sources (Sherman, 1991). Yeast strains used in this study are summarized in Table 1. Strains KN4083 (*cdc4–1*; Dr. K. Nasmyth, IMP, Vienna, Austria), KN1416 (*cdc7–1*, Dr. K. Nasmyth), K1414 (*cdc28–4*, Dr. M. Hall, Biocenter, Basel, Switzerland), 381GG28a6 (*cdc28–13*, Yeast Genetic Stock Centre) and Mx161–3a (*mps1–1*, Dr. M. Winey, University of Colorado, Boulder, CO) were back crossed three times against strains YPH500 or YPH499 (Sikorski and Hieter, 1989), resulting in strains GPY52, GPY30, GPY31, GPY32, and GPY48, respectively. GPY54–1 and GPY54–3 were constructed by disruption of the *SST1/BAR1* gene using the Δ*sst1::URA3* cassette of plasmid pJG-*sst1* (Reneke *et al.*, 1988) in strains GPY52 and YPH499. Strains ESM364, ESM374, ESM376, ESM380, ESM383, ESM385, and ESM389 were constructed as follows. CB018 was transformed with the linearized plasmid pGP50 (*Pst*I; pRS306-*Gal1-SPC98*) using the lithium-acetate method (Schiestl and Gietz, 1989). Transformants (ESM364) were selected on SC medium lacking uracil. The integration of the *Gal1-SPC98* gene fusion at the *URA3* locus provides a *Gal1-SPC98* flanked by *ura3–1* and *URA3*. CB018 and ESM364 were then transformed with pMK122 (pRS305-*Gal1-TUB4*) previously restricted with *Bst*EII. This resulted in the integration of *Gal1-TUB4* into the *LEU2* locus of CB018 or ESM364. The transformants were named ESM376 and ESM374. Finally, pMK123 (pRS304-*Gal1-SPC97–3HA*) was linerized with *Bsg*I and transformed into CB018, ESM364, ESM374, and ESM376 to give strains ESM380, ESM383, ESM389, and ESM385, respectively. Transformants were selected on SC plates lacking tryptophan. Strain GPY42 (*SPC97–3HA*) was obtained by transforming cells of CB018 with linearized pMK120. Transformants were selected on SC plates lacking tryptophan. These contain *SPC97–3HA* flanked by the *TRP1* gene.

Plasmids

Plasmids used in this study are summarized in Table 1. Plasmids pGP20, pGP22, pGP27, pGP31, and pSM456, containing *3HA-spc98*[nls1] to *3HA-spc98*[nls5] in pRS315, were constructed by recombinant polymerase chain reaction (PCR) using the oligonucleotides described in Table 2. PCR was performed with Vent polymerase (New England Biolabs, Beverly, MA). The nucleotide sequence of PCR products was determined by the chain termination method (Sanger *et al.*, 1977). In detail, for the deletion of the codons 580–595 of *SPC98*, plasmid pSM276 (*SPC98* in pBlue SK) (Geissler *et al.*, 1996) was submitted to PCR using the oligonucleotides SPC90–2/NLS2 and M13rev/NLS1 (Table 2). The PCR products of 1760 base pairs (bp) and 1122 bp were purified, mixed, and submitted to an additional PCR using primers M13rev/SPC90–2. The 3750-bp product was restricted with *Apa*I-*Sac*I and cloned into the *Apa*I-*Sac*I sites of pRS315, creating plasmid pNLS1 (*spc98*[nls1]). The 1766-bp *Hind*III fragment of pNLS1, containing the deletion, was then ligated into

the 7778-bp *Hin*dIII fragment of pSM338 (*3HA-SPC98* in pRS315). The resulting plasmid was named pGP20 (*3HA-spc98*nls1 in pRS315). Plasmid pGP22 (*3HA-spc98*nls2 in pRS315) was constructed by recombinant PCR using pSM338 as template and the primers M13–24rev/MNLS2 and MNLS1/M13–24hin. The two PCR products of 2201 bp and 1717 bp were mixed and resubmitted to another PCR using M13–24rev/M13–24hin. The 3878-bp product was restricted with *Apa*I-*Sac*I and cloned into pRS315 previously restricted with the same enzymes. Plasmid pGP27 (*3HA-spc98*nls3 in pRS315) was constructed as pGP22; however, the primers M13–24rev/MNLS4 and M13–24hin/MNLS3 were used for the first two PCRs. Plasmid pGP31 (*3HA-spc98*nls5 in pRS315) was constructed with the same primers as for pGP27, but using plasmid pGP22 as a template. Similarly, pSM456 (*3HA-spc98*nls4 in pRS315) was obtained by recombinant PCR with pGP22 as a template and the oligonucleotides MNLS5 and MNLS6.

To obtain *SPC98* derivatives under the control of the *Gal1*-promoter, the 1026-bp *Hin*dIII fragment of the *3HA-spc98*nls constructs, carrying the mutated NLS sequence, was ligated with the 8000-bp *Hin*dIII fragment of pSM289 (*SPC98* in pYES2) resulting in the plasmids pGP25, pGP26, pGP29, pSM436, and pGP30, respectively. For construction of *3HA-SPC98* derivatives in the 2-μm plasmid pRS425, plasmids pSM338, pGP20, pGP22, pGP27, pSM456, and pGP31 were restricted with *Sac*I, which released a 3800-bp DNA fragment carrying either *3HA-SPC98*, *3HA-spc98*nls1, *3HA-spc98*nls2, *3HA-spc98*nls3, *3HA-spc98*nls4, or *3HA-spc98*nls5. These fragments were ligated with pRS425 previously restricted with *Sac*I, resulting in plasmids pGP43, pGP44, pGP45, pGP46, pGP58, and pGP47.

NLS-LacZ gene fusions were constructed as described (Geissler *et al.*, 1996), using the 244-bp *Bam*HI-*Xba*I fragment of *SPC98* and *spc98*nls. pSM429 (*Gal1-GST-MPS1*) was constructed as reported by Lauzé *et al.* (1995). *Gal1-SPC98*, *Gal1-TUB4*, and *Gal1-SPC97–3HA* were ligated into yeast integration vectors. In brief, the 4000-bp *Nae*I-*Xho*I fragment of pSM289 (*Gal1-SPC98*) was cloned in the *Sma*I-*Xho*I restriction sites of pRS306 (pGP50). Similarly, the 2600-bp *Nae*I-*Xba*I fragment of pSM209 (*Gal1-TUB4*) (Geissler *et al.*, 1996) was cloned into the *Sma*I-*Xba*I sites of pRS305 to give plasmid pMK122, and the 4500-bp *Sac*I-*Eco*RV fragment of pMK81 (Knop *et al.*, 1997) carrying *Gal1-SPC97–3HA* was ligated into pRS304 restricted with the same enzymes (pMK123). For the construction of pMK120, the 1045-bp *Spe*I-*Apa*I fragment of pMK81 (*SPC97–3HA*) was cloned into the *Spe*I-*Apa*I sites of integration vector pRS304. Subfragments of *SPC98* in the two-hybrid vector pACTII were constructed as described in Table 1. Plasmid pGP48 was constructed by the integration of a 2995-bp *Bgl*II-*Apa*I fragment containing *SPC97* of pMK10 (Knop *et al.*, 1997) into pRS424 previously restricted with *Bam*HI and *Apa*I. *TUB4* on a *Sac*I fragment was then inserted into the *Sac*I restriction site of the polylinker region of pRS424.

Antibodies, Protein Determination, and Immunoblotting

The following antibodies were used: affinity-purified goat and rabbit anti-Spc98p (Geissler *et al.*, 1996; Knop and Schiebel, 1997), affinity-purified goat and rabbit anti-Tub4p (Spang *et al.*, 1996a; Knop *et al.*, 1997), mouse monoclonal 12CA5 antibodies (anti-HA) (Hiss GmbH, Freiburg, Germany), affinity-purified rabbit anti-Spc97p (Knop and Schiebel, 1997), affinity-purified rabbit anti-Spc110p (Spang *et al.*, 1996b), affinity-purified rabbit anti-Spc42p (Knop and Schiebel, 1997), rabbit anti-Fas (kindly provided by Dr. R. Egner, Biozentrum, Vienna, Austria), and rabbit anti-Nop1p (Dr. E. Hurt, University of Heidelberg, Heidelberg, Germany). Mouse monoclonal anti-β-galactosidase antibodies were from Boehringer Mannheim (Mannheim, Germany). Secondary antibodies for the immunoreactions were goat anti-rabbit or goat anti-mouse IgGs conjugated with horse radish peroxidase (Jackson ImmunoResearch Laboratories, West Grove, PA).

Protein concentration was determined by the method of Bradford (1976) using bovine albumin as standard. Proteins were separated by SDS-PAGE (Laemmli, 1970) and transferred onto nitrocellulose membranes (Schleicher & Schuell, Dassel, Germany) using a semidry blotting apparatus from Bio-Rad (Richmond, CA). Blotting was for 2 h with 2 mA/cm². The blotting buffer contained 20% methanol, 0.02% SDS, 25 mM Tris, 192 mM glycine. Nitocellulose membranes were blocked, incubated with the described antibodies, and finally washed following standard protocols (Harlow and Lane, 1988). The immunoreaction was visualized using the ECL kit from Amersham (Arlington Heights, IL).

Immunoprecipitation

Yeast cells were grown in SC or YPD medium to midlogarithmic phase (approximately 2×10^7 cells/ml), harvested by centrifugation, and washed once with cold water. The cells were lysed with glass beads in IP buffer (20 mM Tris-Cl, pH 7.4, 100 mM NaCl, 10 mM EDTA, 1 mM EGTA, 5% glycerol) containing protease inhibitors (6 μg/ml antipain, 4.3 μg/ml leupeptin, 4.5 μg/ml aprotinin, 5 μg/ml bovine trypsin inhibitor, 5 μg/ml pepstatin, 6 μg/ml chymostatin, 350 μg/ml benzamidine-HCl, 1 mM phenylmethylsulfonyl fluoride [PMSF]) (all from Sigma-Aldrich, Deisenhofen; Germany) and phosphatase inhibitors (100 mM 3-glycerophosphate, 50 mM NaF, 0.2 mM Na-monovanadate) (Sigma-Aldrich). After cell lysis (>95%), 1% Triton X-100 was added and the lysate was incubated on ice for 15 min. The suspension was cleared by centrifugation (5,000 × g, 10 min). Cell lysates were incubated with goat anti-Spc98p antibodies, goat anti-Tub4p antibodies, or mouse anti-HA antibodies cross-linked to protein-G Sepharose (Harlow and Lane, 1988) for 4 h at 4°C. The beads were washed three times with IP buffer and finally resuspended in urea (HU) buffer (Knop *et al.*, 1996). Samples precipitated with goat anti-Spc98p or goat anti-Tub4p antibodies were analyzed by immunoblotting using rabbit anti-Spc98p or rabbit anti-Tub4p antibodies, respectively.

Alkaline Phosphatase (AP) and Protein Phosphatase 2A (PP2A) Treatments

Spc98p was immunoprecipitated as described above. The precipitated material was washed twice with AP buffer (150 mM NaCl, 1 mM MgCl₂, 0.1 mM ZnCl₂, 1 mM PMSF, 50 mM Tris-Cl, pH 8.0), resuspended in an equal volume of AP buffer containing 0.4% SDS, and incubated at 65°C for 3 min. After cooling, 10 U of AP (Boehringer Mannheim) were added, and the samples were incubated at 30°C for 45 min. Similarly, isolated SPBs were resuspended in AP buffer with 0.4% SDS, incubated at 65°C for 3 min, and treated with AP. The reactions were stopped by the addition of an equal volume of HU buffer. The samples were heated for 15 min at 65°C. The PP2A treatment was performed in a similar manner, except that the precipitated material was washed with PP buffer (60 μM EGTA, 1 mM MnCl₂, 0.3 mg/ml bovine serum albumin, 0.033% β-mercaptoethanol, 1 mM PMSF, 30 mM Tris-Cl, pH 7.5), heated for 3 min at 65°C, and incubated with 1 mU PP2A from bovine heart (Boehringer Mannheim) for 45 min at 30°C.

In Vivo Labeling of Yeast Cells with [³²P]

Cells of strains YPH499 (*SPC98*) and ESM279 (*3HA-SPC98*) were grown to early logarithmic phase in phosphate-free medium (Rubin, 1973). Cells (3 ml, 1×10^7 cells/ml) were incubated for 4 h at 30°C with 400 μCi of [³²P]orthophosphate (10 mCi/ml; Amersham Buchler, Braunschweig, Germany). The cells were washed three times with cold water and resuspended in 100 μl 50 mM Tris-Cl, pH 7.5, 1 mM EDTA, 1% SDS, containing protease and phosphatase inhibitors as above. Cell lysis was performed at 4°C by strong vortexing with glass beads followed by an incubation for 5 min at 65°C. The samples were centrifuged at 12,000 × g for 3 min, and the supernatant was transferred to a new tube and diluted 20 times with 150 mM NaCl, 1% Triton X-100, 15 mM Tris-Cl, pH 7.5, and 0.1% SDS. After preclearing with protein-G Sepharose (Sigma-Aldrich,

Deisenhofen; Germany) 12CA5 antibodies were added and incubated for 1 h at 4°C, followed by precipitation of the antibodies with protein-G Sepharose for 1 h. To reduce the background, 5 mg of unlabeled protein extract from the wild-type strain (YPH499) were added to the immunoprecipitations, and the protein-G sepharose beads were precoated with buffer containing 1% bovine serum albumin (Sigma-Aldrich). The precipitated material was successively washed with 1) 150 mM NaCl, 1% Triton X-100, 15 mM Tris-Cl, pH 7.5, 0.1% SDS; 2) 2 M urea, 200 mM NaCl, 1% Triton X-100, 100 mM Tris-Cl, pH 7.5; 3) 500 mM NaCl, 1% Triton X-100, 20 mM Tris-Cl, pH 7.5; and 4) 50 mM NaCl, 10 mM Tris-Cl, pH 7.5. The beads were resuspended in an equal volume of HU buffer. The samples were heated at 65°C for 15 min, separated by SDS-PAGE, and blotted onto nitrocellulose membranes. The membrane was first analyzed by autoradiography followed by immunodetection of Spc98p.

In Vitro Phosphorylation Assay

CB018, ESM364 (*Gal1-SPC98*), and ESM389 (*Gal1-SPC98, Gal1-SPC97–3HA and Gal1-TUB4*) strains pregrown in SC-raffinose medium to midlog phase were diluted to an OD_{600} of 0.3 (approximately 0.6×10^7 cells/ml) with SC-raffinose medium. Galactose was added (2%), and the cells were incubated at 30°C for 6 h. Spc98p or Spc98p/Tub4p/Spc97p complex was immunoprecipitated with goat anti-Spc98p antibodies. CB018 cells transformed with pSM429 (*Gal1-GST-MPS1*) or pEG(KT) (*Gal1-GST*) were induced with 4% galactose for 6 h. Glutathione-*S*-transferase (GST)-Mps1p and GST were affinity purified as reported by Lauzé *et al.* (1995) using glutathione Sepharose (Pharmacia, Freiburg, Germany). The kinase assay was performed as described (Lauzé *et al.*, 1995), except that 10 mM glutathione was added to the samples.

Synchronization of Yeast Cells, Flow Cytometry, Hydroxyurea, and Nocodazole Treatments

Cells were synchronized with 1 μg/ml (*sst1/bar1* strains) or 10 μg/ml (*SST1/BAR1* strains) of synthetic α-factor (Sigma-Aldrich) at 30°C or 23°C for approximately 3 h. Cells were released from the cell cycle block by washing them once with prewarmed YPD medium. Cells of strain RH210–3c (*cdc15*) were grown in YPD to 5×10^6 cells/ml at 23°C. The culture was then incubated for 3 h at 37°C. During this time, most of the cells (> 95%) arrested in late anaphase. These cells continued synchronously through the cell cycle when they were further incubated at 23°C. DNA content of cells was determined by flow cytometry as described (Hutter and Eipel, 1979). Cells of YPH499 were treated with 100 mM hydroxyurea (Sigma-Aldrich) or 15 μg/ml nocodazole (Sigma-Aldrich) for 3 h at 30°C. Cells arrested uniformly in the cell cycle (> 95%). Lysates were prepared and Spc98p phosphorylation was analyzed as previously described.

Overexpression of SPC98, spc98[nls], TUB4, SPC97–3HA, NLS-LacZ, and Immunofluorescence

Yeast cells carrying genes under the control of the *Gal1*-promoter were grown to early logarithmic phase (5×10^6 cells/ml) in SC medium containing 2% raffinose as sole carbon source. Galactose (2%) was added for 6 h. Cells were fixed by adjusting the medium to 3.5% formaldehyde and 0.1 M K-phosphate, pH 6.5, for 45 min at 30°C. Immunofluorescence was performed as described (Knop *et al.*, 1997). Affinity-purified rabbit anti-Spc98p, anti-Tub4p, and anti-Spc97p or mouse anti-β-Gal were used as primary antibodies. Secondary antibodies were goat anti-rabbit or goat anti-mouse IgGs conjugated with Cy3 (Jackson ImmunoResearch Laboratories). DNA was stained with 4,6-diamidino-2-phenylindole (DAPI) (Boehringer Mannheim).

Yeast Cytoplasm and Nuclei Fractionation

Fractions containing cytoplasm and nuclei were enriched from the strain GPY42 as described (Young and Tyk, 1997). Briefly, spheroblasts were resuspended in Ficoll buffer (18% Ficoll 400, 20 mM Tris-HCl, pH 7.5, 20 mM KCl, 5 mM $MgCl_2$, 3 mM dithiothreitol, 1 mM EDTA) containing protease and phosphatase inhibitors as described above. The spheroblasts were lysed using a Dounce homogenizer. Unlysed cells and cell debris were removed by two rounds of centrifugation (2,150 × g, 5 min). The supernatant was equally divided in two portions: one was saved as total extract (TE) and the other was centrifuged at high-speed (20,800 × g, 30 min), resulting in a cytosolic supernatant (Cy) and a nuclear pellet (Nu). The pellet was resuspended in Ficoll buffer to the original volume. The fractions (TE, Cy, Nu) were diluted with one volume of 50 mM Tris-HCl, pH 7.5, 10 mM $MgSO_4$, 1 mM EDTA, 10 mM potassium acetate, 1 mM dithiothreitol, and 2% Triton X-100 containing protease and phosphatase inhibitors and treated with 20 U of deoxyribonuclease I for 30 min at 37°C. The samples were then diluted 10 times with IP buffer, and Spc98p was immunoprecipitated as described. Coimmunoprecipitated Tub4p and Spc97p were detected by immunoblotting. Aliquots of TE, Cy, and Nu fractions were also analyzed by immunoblotting using anti-Fas and anti-Nop1p antibodies.

Two-Hybrid Assay, SPB, and Nuclei Isolation and Immunoelectron Microscopy

Two-hybrid assays were performed as reported (Geissler *et al.*, 1996). For nuclei and SPB isolation, we followed the protocol described by Rout and Kilmartin (1990). Immunoelectron microscopy was performed as described (Knop *et al.*, 1997).

RESULTS

Spc98p Is a Phosphoprotein

Previously, we have shown that the yeast γ-tubulin, Tub4p, is in a 6S complex together with the SPB components Spc98p (Geissler *et al.*, 1996) and Spc97p (Knop *et al.*, 1997). This complex is present in the cytoplasm (this study) as well as at the SPB (Rout and Kilmartin, 1990; Spang *et al.*, 1996a; Knop *et al.*, 1997). For the study of the assembly and modification of the Tub4p complex, it was necessary to show that the different forms of the Tub4p complex can be immunoprecipitated with equal efficiency. Yeast cells were lysed and the detergent Triton X-100 was added. This treatment extracted most of the SPB-associated Tub4p complex (Knop and Schiebel, 1997). Consequently, Tub4p, Spc98p, or Spc97p-3HA were not detected in the sediment after centrifugation (Figure 1A, lane 1). Tub4p, Spc98p, and Spc97–3HA of the supernatant were then immunoprecipitated (lane 2). The precipitation was quantitative, since the proteins were no longer detectable in the supernatant after the immunobeads had been removed by centrifugation (lane 3). Taken together, we conclude that the cytoplasmic and SPB-derived forms of the Tub4p complex were precipitated with equal efficiency by our antibodies.

During the course of the immunoprecipitation experiments, we noticed that Spc98p in the Tub4p complex migrates as a heterogeneous group of bands of apparent molecular mass between 98 and 105 kDa

(Figure 1B, lane 1). Such behavior is often a consequence of hyperphosphorylation. This possibility was tested by the incubation of immunoprecipitated Spc98p with AP, which converted the slower migrating forms of Spc98p into mainly one band (Figure 1B, lane 2). However, a slower migrating, minor form of Spc98p was also observed. This band may result from a phosphorylated residue of Spc98p being inaccessible to the phosphatase or from a modification other than phosphorylation. Conversion was blocked when AP was inhibited by the phosphatase inhibitor 3-glycerophosphate (Figure 1B, lane 3). A similar conversion was observed with the phosphoserine/threonine-specific phosphatase PP2A (Figure 1C), suggesting that Spc98p is phosphorylated mainly on serine and threonine residues. Again, this conversion was incomplete, raising the possibility that some Spc98p is also phosphorylated on residues other than serine and threonine.

To confirm the phosphorylation of Spc98p, we labeled yeast cells with [^{32}P]orthophosphate and enriched 3HA-Spc98p by immunoprecipitation using anti-HA antibodies. 3HA-Spc98p was labeled by [^{32}P], demonstrating directly that Spc98p is a phosphoprotein (Figure 1D, lane 2). Noteworthy, only the slower migrating band of Spc98p was detected by autoradiography (compare lanes 2 and 4). We conclude that Spc98p is a phosphoprotein and that the faster migrating form is not, or is only weakly, phosphorylated.

Spc98p Is Phosphorylated in a Cell Cycle-dependent Manner

To test whether Spc98p phosphorylation is cell cycle-dependent, yeast cells were synchronized using α-factor (Figure 2A). Cell cycle progression of the cells was followed by determining the budding index and the DNA content by flow cytometry. In α-factor–arrested cells (t = 0), the ratio of nonphosphorylated to phosphorylated Spc98p was about equal; however, we observed some variation depending on the experiment (Figures 2A and 4A). The phosphorylated form then increased with bud formation (Figure 2A, t = 30 min), was maximal during DNA replication (t = 40 min), and finally reached a minimum in large-budded mitotic cells (t = 70 min). Remarkably, phosphorylation of the SPB component Spc110p (Friedmann *et al.*, 1996; Stirling and Stark, 1996) peaked about 20 min later in the cell cycle (Figure 2A, t = 60 min). To exclude possible artefacts caused by the pheromone arrest, we uniformly arrested *cdc15* cells in anaphase at 37°C (Schweitzer and Philippsen, 1991). Cells continued synchronously through the cell cyle after the temperature was shifted to 23°C (Figure 2B). As before, Spc98p was phosphorylated with bud formation (t = 75 min) and was predominantly nonphosphorylated in large budded mitotic cells (t = 150 min).
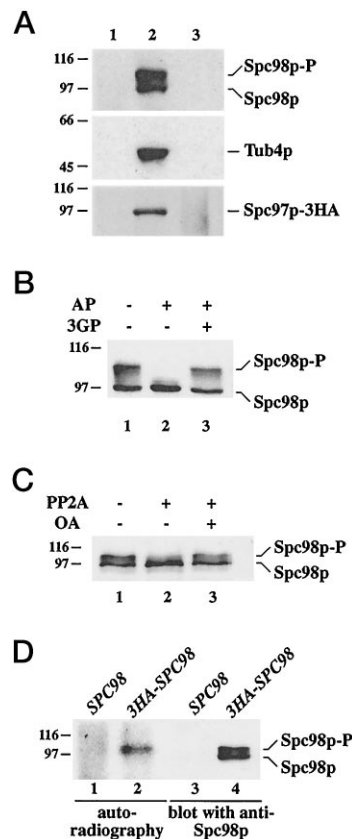

Figure 1. Immunoprecipitation and phosphorylation of Spc98p. (A) Immunoprecipitation of Tub4p, Spc98p, and Spc97p-3HA is quantitative. Yeast cells were lysed with glass beads in the presence of 1% Triton X-100 as described in MATERIALS AND METHODS. The lysate was centrifuged for 5 min at 500 × *g* to remove unlysed cells. The supernatant was then centrifuged (10 min, 5,000 × *g*) to give a pellet (lane 1) and a supernatant. This supernatant was incubated with anti-Tub4p, anti-Spc98p, or anti-HA (Spc97p-3HA) antibodies cross-linked to protein-G Sepharose for 4 h at 4°C. The protein-G beads were collected by centrifugation (lane 2). Proteins in the supernatant were concentrated by trichloroacetic acid (TCA, 10% final concentration) precipitation (lane 3). Comparable aliquots were analyzed by immunoblotting using anti-Tub4p, anti-Spc98p, or anti-HA (Spc97p-3HA) antibodies. (B) Spc98p is a phosphoprotein. Immunoprecipitated Spc98p was incubated without phosphatase (lane 1), or with AP in the absence (lane 2) or in the presence (lane 3) of the inhibitor 3-glycerophosphate (3GP) (100 mM). Spc98p was detected by immunoblotting using goat anti-Spc98p antibodies. (C) Serine or threonine residues of Spc98p are phosphorylated. Spc98p was incubated in buffer only (lane 1), or with the phosphoserine/threonine-specific phosphatase PP2A in the absence (lane 2) or in the presence (lane 3) of 5 μM of the inhibitor okadaic acid (OA). Samples were analyzed by immunoblotting with anti-Spc98p antibodies. (D) In vivo phosphorylation of Spc98p. *SPC98* (lanes 1 and 3) and *3HA-SPC98* (lanes 2 and 4) cells were grown in the presence of [^{32}P]-orthophosphate. Immunoprecipitation was performed with anti-HA antibodies. 3HA-Spc98p was visualized by autoradiography (lanes 1 and 2) and immunoblotting with anti-Spc98p antibodies (lanes 3 and 4). The position of the molecular weight standards β-galactosidase (116 kDa) and phosphorylase b (97 kDa) is indicated. Experimental procedures are described in MATERIALS AND METHODS.

Table 1. Yeast strains-plasmids

Name	Genotype - construction	Source or reference
Yeast strains		
CB018	*MAT***a** *ura3-1 his3-11,15 leu2-3,112 ade2-1 trp1-1 can1-100 Δpep4::HIS3 Δprb1::hisG Δprc1:: hisG*	from R. Fuller, for ref. see Graham and Emr (1991)
ESM243	*MAT***a** *ura3-52 lys2-801 ade2-101 trp1Δ63 his3Δ200 leu2Δ1 Δspc98::HIS3 pSM296*	Geissler *et al.* (1996)
ESM279	*MAT***a** *ura3-52 lys2-801 ade2-101 trp1Δ63 his3Δ200 leu2Δ1 Δspc98::HIS3 pSM338*	Geissler *et al.* (1996)
ESM364	*MAT***a** *his3-11,15 leu2-3,112 ade2-1 trp1-1 can1-100 Δpep4::HIS3 Δprb1::hisG Δprc1::hisG ura3-1::pGP50*	this study
ESM374	*MAT***a** *his3-11,15 ade2-1 trp1-1 can1-100 Δpep4::HIS3 Δprb1::hisG Δprc1::hisG ura3-1::pGP50 leu2-3,112::pMK122*	this study
ESM376	*MAT***a** *ura3-1 his3-11,15 ade2-1 trp1-1 can1-100 Δpep4::HIS3 Δprb1::hisG Δprc1::hisG leu2-3,112::pMK122*	this study
ESM380	*MAT***a** *ura3-1 his3-11,15 leu2-3,112 ade2-1 can1-100 Δpep4::HIS3 Δprb1::hisG Δprc1::hisG trp1-1::pMK123*	this study
ESM383	*MAT***a** *his3-11,15 leu2-3,112 ade2-1 can1-100 Δpep4::HIS3 Δprb1::hisG Δprc1::hisG ura3-1::pGP50 trp1-1::pMK123*	this study
ESM385	*MAT***a** *ura3-1 his3-11,15 ade2-1 can1-100 Δpep4::HIS3 Δprb1::hisG Δprc1::hisG leu2-3,112::pMK122 trp1-1::pMK123*	this study
ESM389	*MAT***a** *his3-11,15 ade2-1 can1-100 Δpep4::HIS3 Δprb1::hisG Δprc1::hisG ura3-1::pGP50 leu2-3,112::pMK122 trp1-1::pMK123*	this study
GPY30	*MAT*α *ura3 lys2 ade2 trp1 his3 leu2 cdc7-1*	this study
GPY31	*MAT*α *ura3 lys2 ade2 trp1 his3 leu2 cdc28-4*	this study
GPY32	*MAT*α *ura3 lys2 ade2 trp1 his3 leu2 cdc28-13*	this study
GPY42	*MAT***a** *ura3-1 his3-11,15 leu2-3,112 ade2-1 trp1-1 can1-100 Δpep4::HIS3 Δprb1::hisG Δprc1::hisG SPC97::pMK120*	this study
GPY48	*MAT***a** *ura3 ade2 trp1 his3 leu2 mps1-1*	this study
GPY52	*MAT***a** *ade2 trp1 leu2 his3 ura3 cdc4-1*	this study
GPY54-1	*MAT***a** *ura3 ade2 trp1 his3 leu2 Δsst1::URA3 cdc4-1*	this study
GPY54-3	*MAT***a** *ura3-52 lys2-801 ade2-101 trp1Δ63 his3Δ200 leu2Δ1 Δsst1::URA3*	this study
RH210-3c	*MAT***a** *ade2-1 his4 trp1 ura3 leu2 cdc15*	Schweitzer and Philippsen (1991)
SGY37	*MAT***a** *trp1 his3 leu2 ura3-52::URA3-lexA-op-LacZ*	Geissler *et al.* (1996)
YPH499	*MAT***a** *ura3-52 lys2-801 ade2-101 trp1Δ63 his3Δ200 leu2Δ1*	Sikorski and Hieter (1989)
YPH500	*MAT*α *ura3-52 lys2-801 ade2-101 trp1Δ63 his3Δ200 leu2Δ1*	Sikorski and Hieter (1989)
YPH501	*MAT***a**/α *ura3-52/ura3-52 lys2-801/lys2-801 ade2-101/ade2-101 trp1Δ63/trp1Δ63 his3Δ200/ his3Δ200 leu2Δ1/leu2Δ1*	Sikorski and Hieter (1989)
Plasmids		
pACTII	2 μm, *LEU2*-based vector carrying the *GAL4* activator domain	Durfee *et al.* (1993)
pEG(KT)	2 μm vector for the expression of *GST* gene fusions under control of the *Gal1* promoter	Mitchell *et al.* (1993)
pEG202	2 μm, *HIS3*-based vector carrying the *LexA* DNA-binding domain	Gyuris *et al.* (1993)
pGP20	*3HA-spc98^{nls1}* in pRS315	this study
pGP22	*3HA-spc98^{nls2}* in pRS315	this study
pGP25	*spc98^{nls1}* in pYES2	this study
pGP26	*spc98^{nls2}* in pYES2	this study
pGP27	*3HA-spc98^{nls3}* in pRS315	this study
pGP29	*spc98^{nls5}* in pYES2	this study
pGP30	*spc98^{nls3}* in pYES2	this study
pGP31	*3HA-spc98^{nls5}* in pRS315	this study
pGP43	*3HA-SPC98* in pRS425	this study
pGP44	*3HA-spc98^{nls1}* in pRS425	this study
pGP45	*3HA-spc98^{nls2}* in pRS425	this study
pGP46	*3HA-spc98^{nls3}* in pRS425	this study
pGP47	*3HA-spc98^{nls5}* in pRS425	this study
pGP48	*TUB4* and *SPC97* in pRS424	this study
pGP50	*Gal1-SPC98* in pRS306	this study
pGP58	*3HA-spc98^{nls4}* in pRS425	this study
pMK16	*SPC97* in pEG202	Knop *et al.* (1996)
pMK120	*Δspc97-3HA* (codon 590-821) in pRS304	this study
pMK122	*Gal1-TUB4* in pRS305	this study
pMK123	*Gal1-SPC97-3HA* in pRS304	this study
pRS304	yeast integration vector carrying *TRP1*	Sikorski and Hieter (1989)
pRS305	yeast integration vector carrying *LEU2*	Sikorski and Hieter (1989)
pRS306	yeast integration vector carrying *URA3*	Sikorski and Hieter (1989)
pRS315	*CEN6, LEU2*-based yeast-*E. coli* shuttle vector	Sikorski and Hieter (1989)
pRS316	*CEN6, URA3*-based yeast-*E. coli* shuttle vector	Sikorski and Hieter (1989)

Table 1. (*Continued*)

Name	Genotype - construction	Source or reference
pRS424	2 μm, *TRP1*-based yeast-*E. coli* shuttle vector	Christianson *et al.* (1992)
pRS425	2 μm, *LEU2*-based yeast-*E. coli* shuttle vector	Christianson *et al.* (1992)
pRS426	2 μm, *URA3*-based yeast-*E. coli* shuttle vector	Christianson *et al.* (1992)
pSG21	*TUB4* in pEG202	Geissler *et al.* (1996)
pSG26	*SPC98* in pACTII	Geissler *et al.* (1996)
pSG30	*Nco*I/*Bam*HI fragment of *SPC98* (codon 147-551) in pACTII	Geissler *et al.* (1996)
pSG31	*Sma*I/*Bgl*II fragment of *SPC98* (codon 1-324) in pACTII	Geissler *et al.* (1996)
pSM289	*SPC98* in pYES2: *Gal1-SPC98*	Geissler *et al.* (1996)
pSM296	*SPC98* in pRS316	Geissler *et al.* (1996)
pSM305	*Gal1-Δspc98* (codon 550-631) in YEp357; *Gal1-Δspc98-LacZ*	Geissler *et al.* (1996)
pSM338	*3HA-SPC98* in pRS315	Geissler *et al.* (1996)
pSM398	*Hinc*II fragment of *SPC98* (codon 511-846) in pACTII	this study
pSM399	*Sca*I-*Xho*I fragment of *SPC98* (codon 705-846) in pACTII	this study
pSM415	*Bam*HI/*Xha*I fragment of *spc98^{nls5}* (codon 550-631) in pSM305	this study
pSM429	*MPS1* in pEG(KT): *Gal1-GST-MPS1*	this study
pSM436	*spc98^{nls4}* in pYES2	this study
pSM456	*3HA-spc98^{nls4}* in pRS315	this study
pYES2	2 μm, *URA3*-based yeast-*E. coli* shuttle vector carrying the *Gal1* promoter	Invitrogen
pYEp357	*URA3* based plasmid carrying the *LacZ* gene	Myers *et al.* (1986)

We investigated the Spc98p phosphorylation in temperature-sensitive kinase mutants that show defects in cell cycle progression or in SPB duplication and mitotic checkpoint control. Phosphorylation of Spc98p was clearly reduced in *cdc28* and *mps1–1* cells, while it was increased in the *cdc7–1* mutant (Figure 3A). Cdc28p is the homolog to Cdc2p of human and *S. pombe* (reviewed by Nasmyth, 1993). Mps1p kinase functions in SPB duplication as well as in mitotic checkpoint control (Winey *et al.*, 1991; Weiss and Winey, 1996; Hardwick *et al.*, 1996). The *cdc7–1* mutation arrests cells before the initiation of DNA replication (Byers and Goetsch, 1974; Hartwell, 1976; Yoon and Campbell, 1991). The phenotype of *mps1–1* cells raised the possibility that Mps1p phosphorylates Spc98p directly. Therefore, we tested whether purified Mps1p phosphorylates Spc98p in vitro (Figure 3B).

We could demonstrate that enriched Spc98p (lane 1) or Spc98p in the Tub4 complex (lane 2) is phosphorylated by purified GST-Mps1p. The Spc98p phosphorylation was dependent on the addition of GST-Mps1p (lanes 1 and 2) and was not observed with purified GST (lanes 4 and 5). As described previously (Lauzé *et al.*, 1995), we noticed that GST-Mps1p is subject to autophosphorylation (lanes 1–3).

The role of Mps1p in checkpoint control (Hardwick *et al.*, 1996; Weiss and Winey, 1996) led us to test whether activation of the DNA replication or the mitotic checkpoint (Hartwell and Weinert, 1989; Hoyt *et al.*, 1991; Li and Murray, 1991; Murray, 1992) influences Spc98p phosphorylation. This was indeed the case, since about 85% of Spc98p of hydroxyurea- or nocodazole-treated cells were phosphorylated (Figure 3, C and D) in comparison to 30% of mitotic cells of a

Table 2. Oligonucleotides used in this study

Name	Sequence
M13rev	5′-GGAAACAGCTATGACCATG-3′
M13-24hin	5′-AGCGGATAACAATTTCACACAGGA-3′
M13-24rev	5′-CGCCAGGGTTTTCCCAGTCACGAC-3′
MNLS1	5′-TAAATCGTCCTTTTGGC<u>TACAGT</u>GAGTATC-3′
MNLS2	5′-AAAATTCGTAGATACT<u>CACTGTA</u>GCCAAAAGG-3′
MNLS3	5′-AATTTTTTATGGG<u>C</u>ATTT<u>GCAGCG</u>AACAAT-3′
MNLS4	5′-GAAATAATTGTT<u>CGCTGC</u>AAATG<u>C</u>CCCATAA-3′
MNLS5	5′-AATTTTTTATGGAGATTT<u>ACAATG</u>AACAAT-3′
MNLS6	5′-GAAATAATTGTT<u>CATTGT</u>AAATCTCCATAA-3′
NLS1	5′-CTTTTGGCAACAATTATTTCTATCAAAGGA-3′
NLS2	5′-CTTTTGATAGAAATAATTGTTGCCAAAAGGACGATTTACGT-3′
SPC90-2	5′-ATGGAACTAGAGCCCACTCT-3′

The basepairs changed to generate the specific mutations in the NLS of *SPC98* (listed in Figure 5A) are underlined.
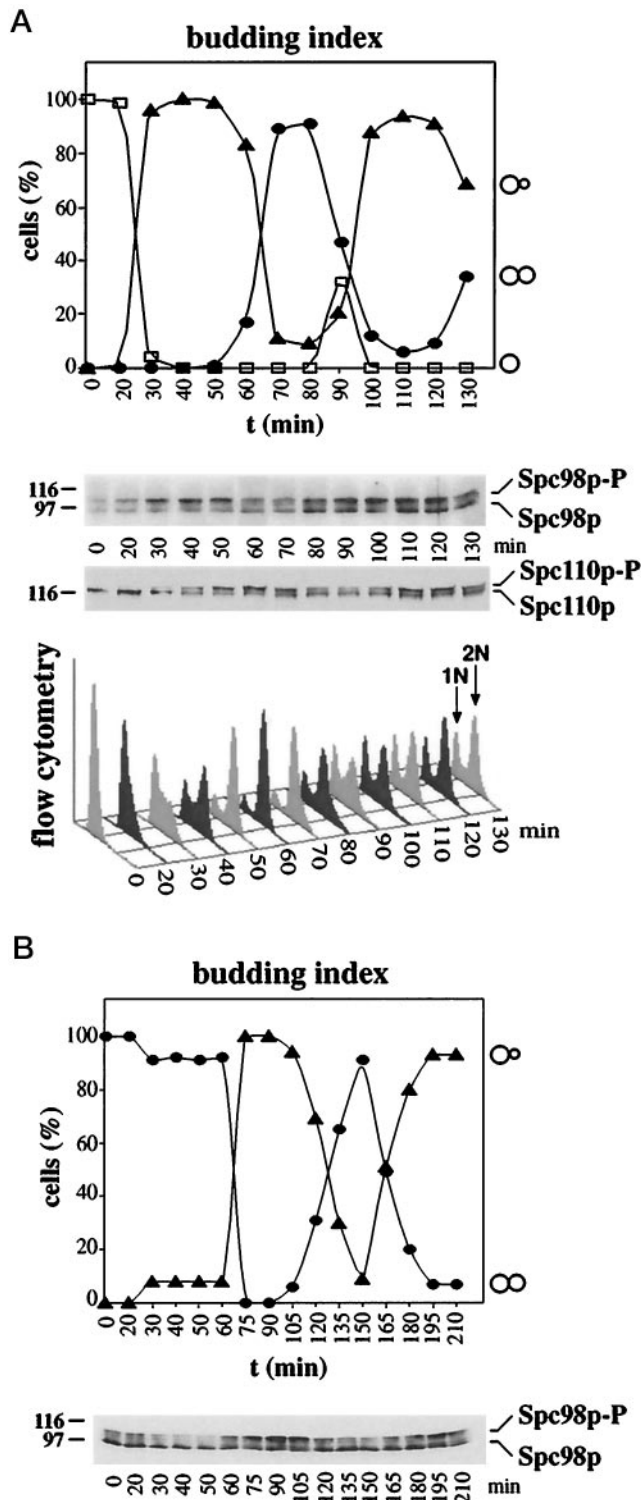
Figure 2. Spc98p is phosphorylated in a cell cycle-dependent manner. (A) A yeast culture (strain YPH499) was synchronized with α-factor. Samples were taken every 10 min after release from the cell cycle block. Cell cycle progression of the culture was followed by determining the budding index. The percentage of unbudded, small

synchronized culture (Figure 2A, t = 70 min; quantified in Figure 3D, mitosis). Taken together, our results show that Spc98p phosphorylation is cell cycle-dependent and that activation of the mitotic and DNA replication checkpoints results in Spc98p phosphorylation.

Spc98p Phosphorylation Is not Required for SPB Duplication or Microtubule Nucleation

Phosphorylation of Spc98p may be a prerequisite for the nucleation of microtubules at the newly formed SPB, since SPB duplication occurs around the time Spc98p phosphorylation begins (Byers and Goetsch, 1974; Byers, 1981). To investigate this important aspect, we made use of the *cdc4−1* mutation. *cdc4−1* cells arrest in the cell cycle before S phase with duplicated but not separated SPBs, and both SPBs are associated with microtubules (Byers and Goetsch, 1974). Therefore, nonphosphorylated Spc98p in arrested *cdc4−1* cells would indicate that this modification does not play a role in SPB duplication or microtubule formation. When α-factor–synchronized *CDC4* cells were shifted to 37°C, these cells replicated their DNA, and Spc98p phosphorylation was observed (Figure 4, A and B). In contrast, *cdc4−1* cells did not replicate their DNA and hyperphosphorylation of Spc98p did not occur (Figure 4, C and D). In summary, the results demonstrate that Spc98p phosphorylation is neither required for SPB duplication nor for nucleating microtubules.

Spc98p Contains an Essential NLS

What is the function of Spc98p phosphorylation? Phosphorylation of Spc98p may regulate the import of Spc98p into the nucleus. Such a regulation has been described for transcription factor Swi5p, which is retained in the cytoplasm through phosphorylation by Cdc28p kinase (Moll *et al.*, 1991). Alternatively, Spc98p phosphorylation may control the assembly of the Tub4p complex, the binding of Tub4p complex to the SPB, or rearrangements of the Tub4p complex after microtubule nucleation. To discriminate between these possibilities, we investigated nuclear import and the assembly of the Tub4p complex.

Figure 2 (cont). budded, and large budded cells (>200) was determined by light microscopy. Spc98p was enriched by immunoprecipitation, and its phosphorylation was analyzed by immunoblotting. Similarly, cell cycle-dependent phosphorylation of Spc110p was followed by immunoblotting (Friedmann *et al.*, 1996). The DNA content was determined by flow cytometry. (B) Synchronization by *cdc15*. *cdc15* cells were shifted to 37°C for 3 h. The uniformly arrested cells were then incubated at 23°C. Samples were taken, and the budding index and Spc98p phosphorylation were analyzed as described in panel A.
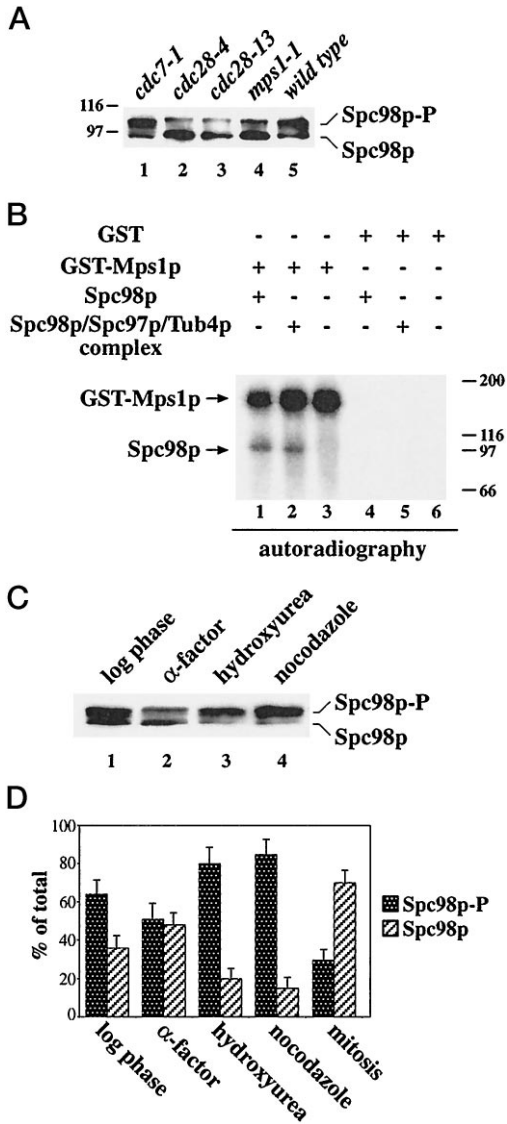
A

B

autoradiography

C

D

A

CDC4 cells

B

C

cdc4-1 cells

D

Figure 4. Spc98p is phosphorylated after SPB duplication. Wild-type (*CDC4*) (A and B) and *cdc4–1* cells (C and D) were synchronized with α-factor at 23°C and then shifted to 37°C in the absence of α-factor. Spc98p of cell lysates was enriched by immunoprecipitation. Spc98p phosphorylation (A and C) was analyzed by immunoblotting using anti-Spc98p antibodies. The DNA content (B and D) of the cells was analyzed over time by flow cytometry.

Figure 3. Spc98p phosphorylation is reduced in *cdc28* and *mps1–1* cells and increased after checkpoint activation. (A) Cells of *cdc7–1* (lane 1), *cdc28–4* (lane 2), *cdc28–13* (lane 3), *mps1–1* (lane 4), and wild type (lane 5) were shifted to 37°C for 4 h. After cell lysis, Spc98p was immunoprecipitated and analyzed by immunoblotting. (B) Mps1p phosphorylates Spc98p in vitro. GST-Mps1p (lanes 1 to 3) or GST (lanes 4 to 6) were isolated from yeast cells using glutathione Sepharose as described (Lauzé *et al.*, 1995). The purified proteins were incubated with buffer (lanes 3 and 6) or immunoprecipitated Spc98p from a strain overexpressing *SPC98* (lanes 1 and 4), or *SPC98*, *SPC97*, and *TUB4* simultaneously (lanes 2 and 5) in the presence of [γ-32P]ATP. Labeled proteins were visualized by autoradiography. Myosin (200 kDa), β-galactosidase (116 kDa), phosphorylase b (97 kDa), and bovine serum albumin (66 kDa) were used as molecular standards. (C) Checkpoint activation increases Spc98p phosphorylation. Spc98p of logarithmic growing cells (lane 1) or of cells treated with α-factor (lane 2), hydroxyurea (lane 3), or nocodazole (lane 4) was immunoprecipitated and then analyzed by immunoblotting. (D) The ratio of phosphorylated to unphosphorylated Spc98p of logarithmic growing cells, or of cells arrested with α-factor, hydroxyurea, or nocodazole, or of mitotic cells of a syn-
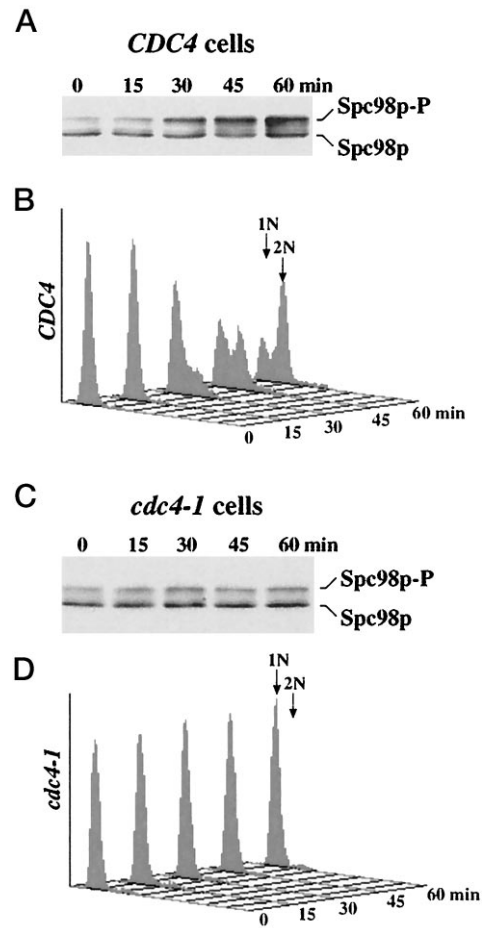
Previously, we have identified a NLS of Spc98p between amino acids 550- 631 (Geissler *et al.*, 1996). Particularly, amino acids 580–595 correspond to a bipartite NLS (Figure 5A) with two clusters of positively charged amino acids separated by a spacer of 10 amino acids (Dingwall and Laskey, 1991). To confirm that this sequence is the NLS of Spc98p, we mutated the putative NLS as indicated in Figure 5A. Mutations in one of the two positively charged clusters of the NLS (Spc98p[nls2] and Spc98p[nls3]) did not affect viability

Figure 3 (cont). chronized culture (see Figure 2A; [t = 70 min]) was quantified by densitometric scanning of the blots using the NIH image program. Shown is the average of three independent experiments. The bars indicate the variation of the experiments.
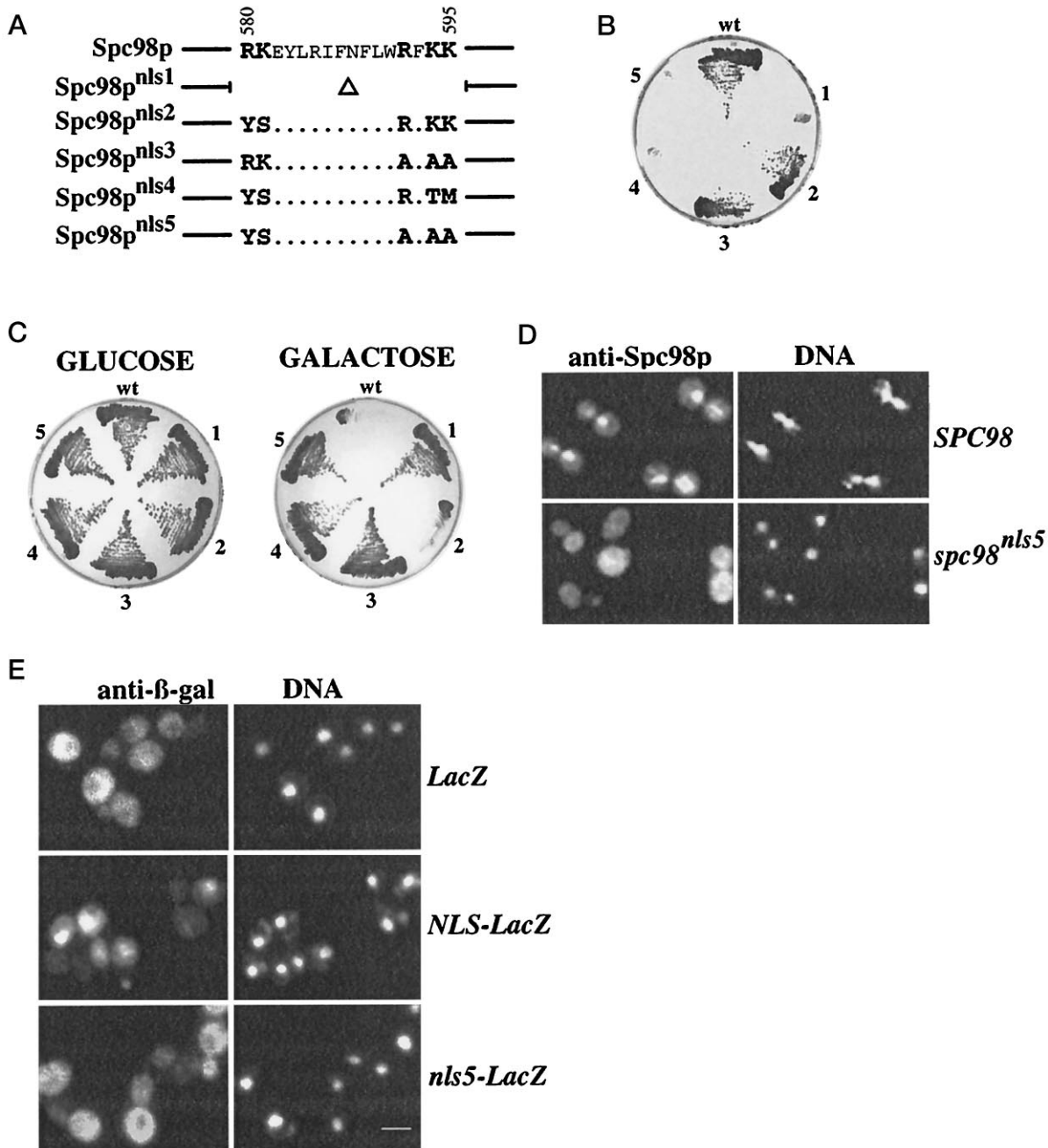
Figure 5. Spc98p contains an essential NLS. (A) Outline of the mutations in the bipartite NLS of Spc98p. Mutations were introduced by recombinant PCR as described in MATERIALS AND METHODS. (B) The NLS of Spc98p is essential for its function. The functionality was determined by a plasmid shuffle experiment using the yeast strain ESM243 (Δ*spc98::HIS3* pRS316-*SPC98*). Cells of ESM243 do not grow on 5-FOA plates at 23°C, which select against the *URA3*-plasmid (Geissler *et al.*, 1996). However, these cells were able to grow on 5-FOA when *LEU2*-based plasmids were present carrying *3HA-SPC98* (pSM338; sector wt), *3HA-spc98*[nls2] (pGP22; sector 2), or *3HA-spc98*[nls3] (pGP27; sector 3). In contrast, *3HA-spc98*[nls1] (pGP20; sector 1), *3HA-spc98*[nls4] (pSM456; sector 4), or *3HA-spc98*[nls5] (pGP31; sector 5) on a *LEU2*-based plasmid did not support growth, revealing that they are nonfunctional. (C) Mutations in the NLS of Spc98p prevent toxicity of *SPC98* overexpression. Strain YPH499 carrying plasmids pSM289 (*Gal1-SPC98,* wt), pGP25 (*Gal1-spc98*[nls1], sector 1), pGP26 (*Gal1-spc98*[nls2], sector 2), pGP30 (*Gal1-spc98*[nls3], sector 3), pSM436 (*Gal1-spc98*[nls4], sector 4), or pGP29 (*Gal1-spc98*[nls5], sector 5) were grown in SC medium with 2% raffinose as carbon source at 30°C to a cell density of 2×10^7 cells/ml. The cells were streaked out on SC plates containing either 2% glucose (no induction of the *Gal1* promoter) or 2% galactose/raffinose (induction). The plates were incubated at 30°C. (D) Mutations in the bipartite NLS of Spc98p impair its nuclear import. *SPC98* and *spc98*[nls5] were expressed from the *Gal1* promoter in wild-type cells (YPH499). Localization of Spc98p was determined by indirect immunofluorescence using affinity-purified anti-Spc98p antibodies. DNA was stained with DAPI. (E) The

(Figure 5B, sectors 2 and 3). In contrast, mutating both clusters (sectors 4 and 5) or the deletion of the NLS (sector 1) resulted in nonfunctional Spc98p^{nls4}, Spc98p^{nls5}, and Spc98p^{nls1} proteins (Figure 5B). Overproduction of Spc98p^{nls1}, Spc98p^{nls3}, Spc98p^{nls4}, or Spc98p^{nls5} was no longer toxic compared with Spc98p or Spc98p^{nls2} (Figure 5C; compare glucose [repression] with galactose [induction]; Geissler *et al.*, 1996) and the overproduced Spc98p^{nls5} accumulated in the cytoplasm of cells (Figure 5D), demonstrating that the NLS was inactivated. This was confirmed by fusing codons 550–631 of *SPC98* and *spc98*^{nls5} to *LacZ* coding for β-galactosidase (β-Gal). β-Gal accumulates in the cytoplasm when expressed in yeast cells (Figure 5E). In contrast, NLS-β-Gal was imported into the nucleus (Geissler *et al.*, 1996), while nls5-β-Gal stayed mainly in the cytoplasm (Figure 5E).

The failure of Spc98p^{nls1}, Spc98p^{nls4}, and Spc98p^{nls5} to function may be caused by protein degradation, by the incapability to form complexes with Tub4p and Spc97p, or by a defect in nuclear import. Epitope-tagged variants (3HA) of *SPC98* or the *spc98*^{nls} mutants were used to discriminate between these possibilities. We established that *3HA-spc98*^{nls4} and *3HA-spc98*^{nls5} were expressed similarly to *3HA-SPC98* and that the proteins were still able to form complexes with Tub4p and Spc97p (Figure 6A, lanes 2, 6, and 7). In contrast, 3HA-Spc98p^{nls1} was impaired in complex formation (lane 3). Furthermore, we noticed that 3HA-Spc98p^{nls1}, 3HA-Spc98p^{nls4}, and 3HA-Spc98p^{nls5} were not phosphorylated (Figure 6A, lanes 3, 6, and 7), while 3HA-Spc98p, 3HA-Spc98p^{nls2}, and 3HA-Spc98p^{nls3} (lanes 2, 4 and 5) were. Noteworthy, after moderate overexpression (2 μm plasmids) of *3HA-spc98*^{nls4} or *3HA-spc98*^{nls5}, but not of *3HA-spc98*^{nls1}, together with similarly overexpressed *TUB4* and *SPC97*, we observed phosphorylation of some 3HA-Spc98p^{nls4} and 3HA-Spc98p^{nls5} (Figure 6B, lanes 6 and 7), indicating that the mutations did not abolish the capability for phosphorylation per se. Under this condition, *spc98*^{nls4} and *spc98*^{nls5} are able to rescue a *SPC98* deletion at 23°C but not at higher temperatures (Figure 6C). These observations are explained by an increase in Spc98p^{nls4} and Spc98p^{nls5} containing Tub4p complexes that probably enter the nucleus with low efficiency.

Spc98p^{nls4} and Spc98p^{nls5} should be located at the outer plaque of the SPB, if they are only defective in nuclear import. This was addressed by examining the localization of 3HA-Spc98p, 3HA-Spc98p^{nls4}, and 3HA-Spc98p^{nls5} at the SPB using immunoelectron microscopy. 3HA-Spc98p^{nls4} and 3HA-Spc98p^{nls5} were only detected at the cytoplasmic outer plaque of the SPB, while 3HA-Spc98p was associated with the inner and outer plaques (Figure 6D; Rout and Kilmartin, 1990). In contrast, SPBs from *SPC98* cells were not labeled by anti-HA antibodies, indicating that the anti-HA signal obtained in the *3HA-SPC98* cells was specific. Taken together, our data are consistent with the notion that Spc98p^{nls4} and Spc98p^{nls5} lost their biological activity mainly due to inactivation of the NLS.

Spc97p and Tub4p Are Imported into the Nucleus in Complex with Spc98p

We investigated nuclear import and complex formation of Spc98p, Tub4p, and Spc97p after overproduction from chromosomally integrated *Gal1-SPC98*, *Gal1-TUB4*, and *Gal1-SPC97* constructs. In contrast to Spc98p (Figure 7A; Geissler *et al.*, 1996), overproduced Tub4p (Figure 7B) or Spc97p (Figure 7C; Knop *et al.*, 1997) were not enriched in the nucleus, suggesting that these proteins do not contain a NLS. However, Tub4p or Spc97p co-overproduced with Spc98p accumulated in the nucleus (Figure 7, B and C), which is indicated by the colocalization of the anti-Tub4p and anti-Spc97p signals with the DAPI staining regions, while co-overproduced Tub4p and Spc97p were enriched in the cytoplasm (Figure 7, B and C). Finally, triple-overproduction of Tub4p, Spc97p, and Spc98p led to the detection of all three proteins inside the nucleus (Figure 7, A, B, and C).

These results are consistent with the notion that Tub4p and Spc97p form complexes with Spc98p in the cytoplasm, which are then imported into the nucleus via the NLS of Spc98p. In this case, complexes of the co-overproduced proteins should be detectable. Immunoprecipitation experiments showed that co-overproduced Tub4p and Spc98p, Tub4p and Spc97p, Spc97p and Spc98p, and triple-overproduced Tub4p, Spc98p, and Spc97p formed complexes (Figure 8A), confirming the mutual interaction of the three proteins that has been suggested by two-hybrid interactions (Geissler *et al.*, 1996; Knop *et al.*, 1997). Remarkably, Spc98p in these complexes was mainly in its unphosphorylated form, suggesting that phosphorylation of Spc98p is neither required for complex formation nor for nuclear import.

Binding of Spc98p to Tub4p and Spc97p raises the possibility that Spc98p has at least two domains, one that binds to Tub4p and another that interacts with Spc97p. This notion is supported by the finding that the C-terminal domain of Spc98p specifically interacts with Tub4p in the two-hybrid system, while the central domain gives a positive signal with Spc97p (Fig-

---

Figure 5 (facing page). mutated NLS is inactive for nuclear import. *LacZ*, *NLS-LacZ*, and *nls5-LacZ* gene fusions were expressed in yeast from the *Gal1* promoter. *LacZ* gene products (β-Gal) were detected by immunofluorescence with monoclonal anti-β-Gal antibodies. DNA was stained with DAPI. Bars in panels D and E are 5 μm.
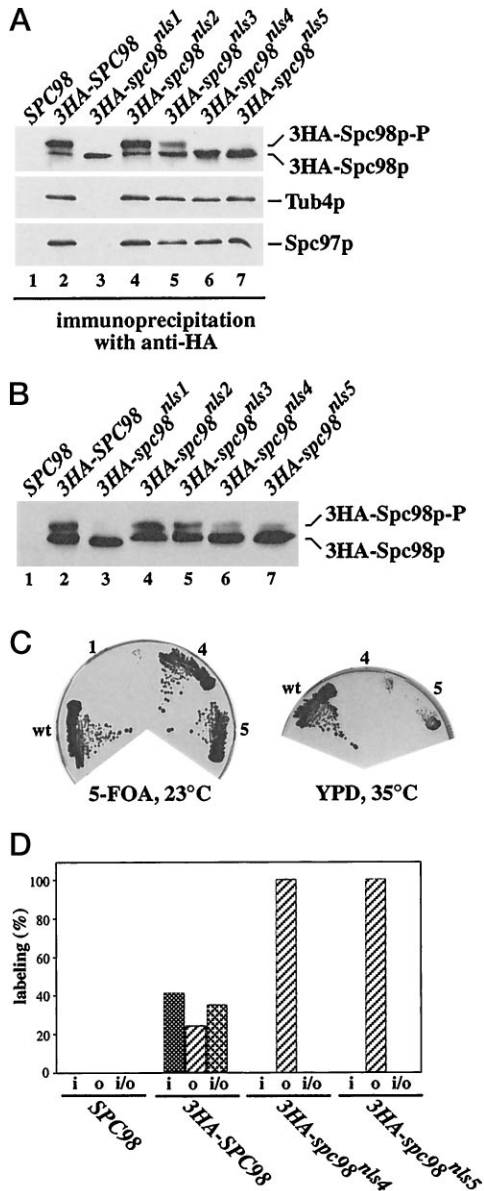
A

immunoprecipitation
with anti-HA

B

C

5-FOA, 23°C   YPD, 35°C

D

Figure 6. The cytoplasmic Spc98p[nls4] and Spc98p[nls5] are not hyperphosphorylated and associate with the outer plaque of the SPB. (A) 3HA-Spc98p[nls4] and 3HA-Spc98p[nls5] form complexes with Tub4p and Spc97p. Proteins of cells expressing *SPC98* only (lane 1), or *SPC98* together with either *3HA-SPC98* (pSM338), *3HA-spc98[nls1]* (pGP20), *3HA-spc98[nls2]* (pGP22), *3HA-spc98[nls3]* (pGP27), *3HA-spc98[nls4]* (pSM456), or *3HA-spc98[nls5]* (pGP31) (lanes 2–7) were precipitated using anti-HA antibodies. Spc98p, Spc97p, and Tub4p were detected in the precipitate by immunoblotting using affinity-purified polyclonal anti-Spc98p, anti-Tub4p, or anti-Spc97p antibodies. (B) Spc98p[nls4] and Spc98p[nls5] can become phosphorylated. Extracts of cells of ESM243 (Δ*spc98::HIS3* pRS316-*SPC98*) carrying plasmid pRS425 (lane 1), pGP43 (*3HA-SPC98*), pGP44 (*3HA-spc98[nls1]*), pGP45 (*3HA-spc98[nls2]*), pGP46 (*3HA-spc98[nls3]*), pGP58 (*3HA-spc98[nls4]*), or pGP47 (*3HA-spc98[nls5]*) (lanes 2–7) were prepared, followed by immunoprecipitation using anti-HA antibodies. The precipitates were analyzed by immunoblotting using polyclonal anti-Spc98p antibodies. These cells carried in addition *SPC97* and

ure 8B). In conclusion, our results suggest that Spc98p has binding sites for Tub4p and Spc97p, and that these interactions are important for the nuclear import of Spc97p and Tub4p.

Spc98p at the Inner but Not the Outer Plaque of the SPB Becomes Phosphorylated

The results of the co-overexpression experiment is most consistent with the view that the Tub4p complex assembles in the cytoplasm followed by its nuclear import. In this case the Tub4p complex should be detectable in the cytoplasm of the cells. The cytoplasm and nuclei of yeast cells were carefully enriched in the presence of phosphatase inhibitors. The distribution of the α- and β-subunits of cytoplasmic fatty acid synthase (Fas) and the nuclear protein nucleolin (Nop1p) established that the two fractions were hardly contaminated by each other (Figure 9A, lanes 1–3). Spc98p was then precipitated using anti-Spc98p antibodies, followed by the immunodetection of Spc98p, Tub4p, and Spc97p-3HA (Figure 9A, lanes 4–6). Coimmunoprecipitation of Tub4p and Spc97p-3HA with anti-Spc98p antibodies demonstrated that the cytoplasmic Spc98p was in complex with Tub4p and Spc97p-3HA (lane 5). Spc98p in the cytoplasmic Tub4p complex was hardly phosphorylated, a result that is consistent with the nonphosphorylation of the import-defective mutants Spc98p[nls4] and Spc98[nls5] (Figure 6A). Spc98p in the nuclear fraction was also associated with Tub4p and Spc97p; however, in contrast to the cytoplasmic Tub4p complex, Spc98p was predominantly phosphorylated (Figure 9A, lane 6).

We investigated whether Spc98p at the SPB is phosphorylated. Isolated nuclei were lysed in the presence of phosphatase inhibitors, followed by the enrichment of SPBs by sucrose density centrifugation (Rout and Kilmartin, 1990). The sucrose gradient fractions were analyzed by immunoblotting for the SPB proteins

Figure 6 (cont). *TUB4* on the 2-μm plasmid pGP48. (C) Spc98p[nls4] and Spc98p[nls5] become functional after overproduction. Cells of strain ESM243 with plasmids pGP48 and either pGP43 (*3HA-SPC98*; sector wt), or pGP44 (*3HA-spc98[nls1]*, sector 1), or pGP58 (*3HA-spc98[nls4]*, sector 4) or pGP47 (*3HA-spc98[nls5]*, sector 5) were grown on 5-FOA at 23°C. 5-FOA selects against the cells carrying the plasmid pRS316-*SPC98*. Growth on this plate indicates that the *SPC98* derivative is functional. Cells from the 5-FOA plate were streaked out on a YPD plate. Cells with *3HA-SPC98* (sector wt) grew, while *3HA-spc98[nls4]* (sector 4) and *3HA-SPC98[nls5]* (sector 5) cells failed to grow at 35°C, but grew at 23°C (our unpublished result). (D) 3HA-Spc98p[nls4] and 3HA-Spc98p[nls5] are associated with the outer plaque of the SPB. Cells expressing *SPC98* or *SPC98* together with *3HA-SPC98*, *3HA-spc98[nls4]*, or *3HA-spc98[nls5]* were prepared for immunoelectron microscopy using anti-HA antibodies as described (Knop *et al.*, 1997). The distribution of gold particles associated with 25 SPBs was determined in each case. The HA signal was associated with the inner (i), outer (o), or inner and outer (i/o) plaques but not with other SPB substructures.
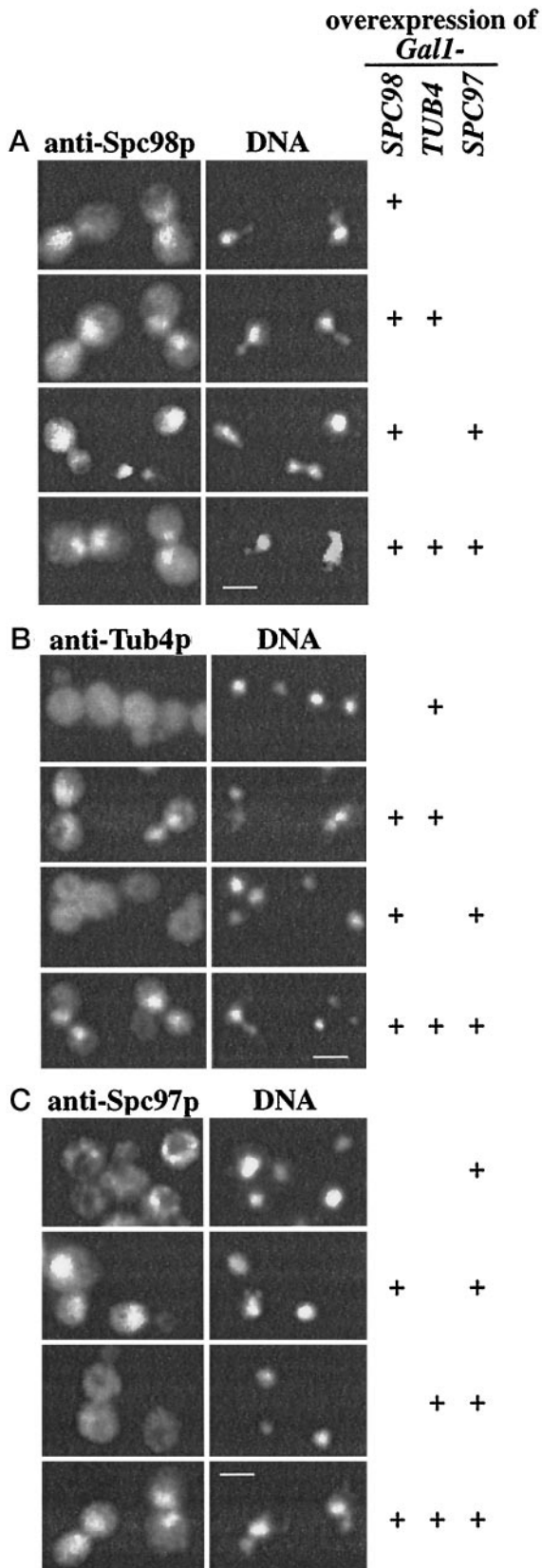
Figure 7.

Spc98p, Spc110p, Spc97p, Tub4p, and Spc42p. Phosphorylated and nonphosphorylated Spc98p comigrated with the other SPB markers (Figure 9B, lanes 8–11). Phosphorylated Spc98p was clearly the predominant form in the SPB fractions. We estimated the ratio of phosphorylated to nonphosphorylated Spc98p of nuclei and isolated SPBs by the scanning of the immunoblots. This ratio increased from nuclei to isolated SPBs by about 1.5- to 2.0-fold, suggesting a pool of nonphosphorylated Spc98p in the nucleoplasm.

We addressed the question whether Spc98p at the outer and inner plaques of the SPB is differently phosphorylated. 3HA-Spc98p^{nls5}, which is predominately associated with the outer plaque of the SPB (Figure 6D), was used for this experiment. Analysis of sucrose gradient fractions 8–11 containing isolated SPBs revealed that 3HA-Spc98p^{nls5} migrated as a single band (Figure 10A, lanes 9–12, detection with anti-HA), while 3HA-Spc98p (lanes 5–8, detection with anti-HA) appeared as a doublet. Migration of 3HA-Spc98p^{nls5} on the gel was not influenced by AP, suggesting that 3HA-Spc98p^{nls5} of isolated SPBs is not phosphorylated (Figure 10B, lanes 3 and 4). In contrast, the migration of 3HA-Spc98p from isolated SPBs was affected by phosphatase treatment (Figure 10B, lanes 1 and 2). Taken together, our results suggest that Spc98p at the inner plaque of the SPB is subject to hyperphosphorylation, while Spc98p at the outer plaque is not.

DISCUSSION

Assembly and Nuclear Import of the Yeast γ-Tubulin Complex

Complexes containing γ-tubulin and homologs of Spc98p have been detected not only in yeast but also in *Drosophila*, human and *X. laevis* (Zheng *et al.*, 1995; Geissler *et al.*, 1996; Moudjou *et al.*, 1996; Knop *et al.*, 1997; Knop and Schiebel, 1997; Murphy and Stearns, personal communication; Zheng, personal communication). These complexes are present in the cytoplasm of cells (Figure 9A; Stearns and Kirschner, 1994; Zheng *et al.*, 1995; Moudjou *et al.*, 1996; Akashi *et al.*, 1997) and are then recruited to the centrosome where they function in microtubule nucleation (Moritz *et al.*, 1995a,b; Knop *et al.*, 1997; Knop and Schiebel, 1997).

Figure 7 (cont). Tub4p and Spc97p are imported into the nucleus via Spc98p. *TUB4*, *SPC98*, and *SPC97* under control of the *Gal1* promoter were integrated into chromosomal locations. The *Gal1* promoters of these strains (see Table 1) were induced for 6 h with galactose. The cellular distribution of overproduced (A) Spc98p, (B) Tub4p, and (C) Spc97p alone or in all possible combinations (as indicated on the right side of Figure 7) was determined by indirect immunofluorescence using affinity-purified polyclonal anti-Spc98p, anti-Tub4p, and anti-Spc97p antibodies. DNA was stained with DAPI. Bars in A, B, and C are 4 μm.
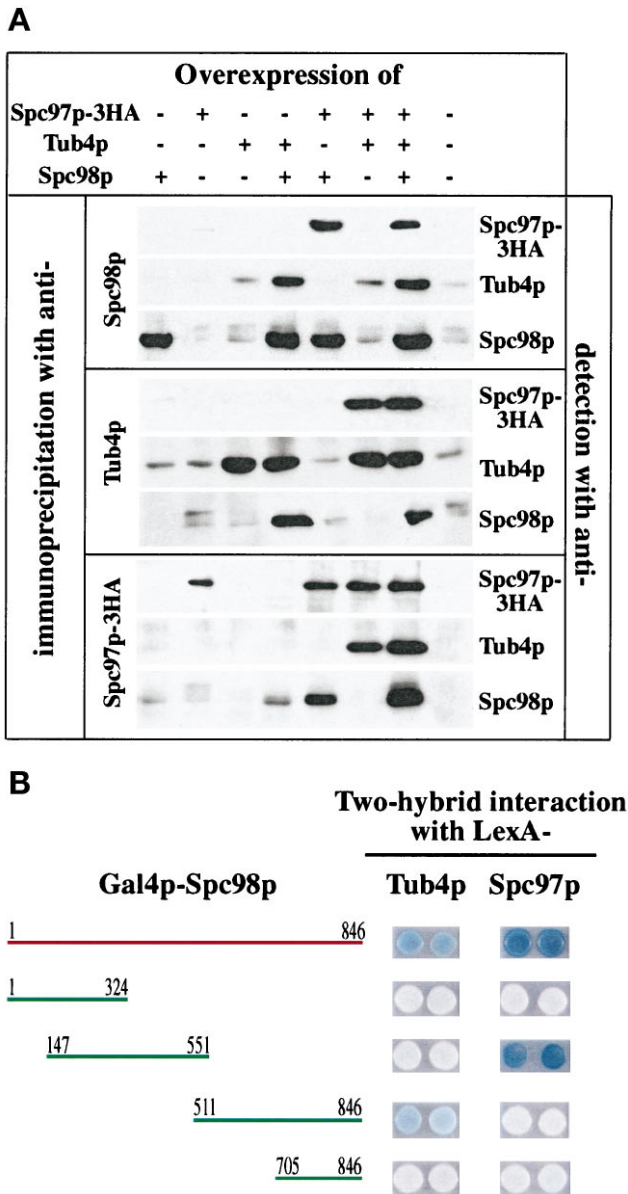
A

B

Figure 8. Overexpressed Tub4p, Spc98p, and Spc97p proteins interact. (A) Overexpressed Tub4p, Spc98p, and Spc97p-3HA form complexes. Tub4p, Spc98p, or Spc97p-3HA from cells expressing *TUB4*, *SPC98*, and *SPC97–3HA* in all possible combinations were enriched by immunoprecipitation using the indicated antibodies. Tub4p, Spc98p, and Spc97p-3HA in the immunoprecipitates were detected by immunoblotting using polyclonal anti-Tub4p, anti-Spc98p, or monoclonal anti-HA (12CA5) antibodies. (B) The central domain of Spc98p interacts with Spc97p, while the carboxy-terminal domain binds to Tub4p. Subclones of Spc98p fused to Gal4p were tested for interaction with LexA-Spc97p and LexA-Tub4p using the two-hybrid system. We established that Gal4p-Spc98p$^{147–551}$ and Gal4p-Spc98p$^{511–846}$ combined with vector pEG202 did not give a positive signal (our unpublished result).

However, it is important to note that the Tub4p complex is, in some respects, distinct from the *X. laevis*

γ-tubulin ring complex. In comparison to the Tub4p complex, the *X. laevis* γ-tubulin complex is larger in size, contains more subunits, and does not need to enter the nucleus for its function (Zheng *et al.*, 1995).

In this study we addressed the question of how a γ-tubulin complex is assembled and regulated using the yeast *S. cerevisiae* as a model system. In yeast, the Tub4p complex is associated with the inner and outer plaques of the SPB (Rout and Kilmartin, 1990; Geissler *et al.*, 1996; Knop *et al.*, 1997), the SPB substructures that organize the nuclear and cytoplasmic microtubules, respectively (Byers and Goetsch, 1974; Byers, 1981). Since the outer plaque is located in the cytoplasm and the inner plaque inside the nucleus, a portion of the components of the Tub4p complex must be transported into the nucleus. Our results are consistent with the view that the Tub4p complex assembles in the cytoplasm and is then imported into the nucleus via the essential NLS of Spc98p (Figure 11). First, the Tub4p complex was detected in the cytoplasm by fractionation studies (Figure 9A). Second, neither Spc97p nor Tub4p seem to have a NLS. Instead, they become imported into the nucleus when cooverexpressed with Spc98p (Figure 7). Third, mutations in the NLS of Spc98p impair its biological function most probably due to insufficient nuclear localization of the protein, since Spc98p^{nls4} and Spc98p^{nls5} assemble in the Tub4p complex (Figure 6A) and become incorporated into the outer plaque (Figure 6D).

Regulatory events must ensure that sufficient Tub4p complex stays in the cytoplasm to enable microtubule nucleation at the outer plaque. Either nuclear import of the Tub4p complex is inefficient or retention proteins, as in the case of NF-κB (Henkel *et al.*, 1992), ensure the maintenance of enough complex in the cytoplasm. Alternatively, phosphorylation could either retain Spc98p in the cytoplasm, as reported for Swi5p (Moll *et al.*, 1991), or trigger its nuclear import. However, our results suggest that Spc98p phosphorylation does not have any of these functions. Phosphorylation of Spc98p does not play a role in its cytoplasmic retention, since the cytoplasmic Tub4p complex contains mainly unphosphorylated Spc98p (Figure 9A). Furthermore, overproduced Spc98p enters the nucleus in its unphosphorylated form, demonstrating that phosphorylation of Spc98p is not required for its nuclear import (Figures 7A and 8A). However, phosphorylation of Spc98p could release a cytoplasmic retention protein followed by the rapid import of Spc98p. This is also unlikely, since in such a scenario phosphorylated Spc98p^{nls} mutants should accumulate in the cytoplasm, which is not the case (Figure 6A). It proved technically difficult to determine the amount and phosphorylation state of Spc98p in the nucleoplasm of wild-type cells, mainly because the Tub4p complex is released easily from the inner plaque of the SPB (Knop and Schiebel, 1997). How-
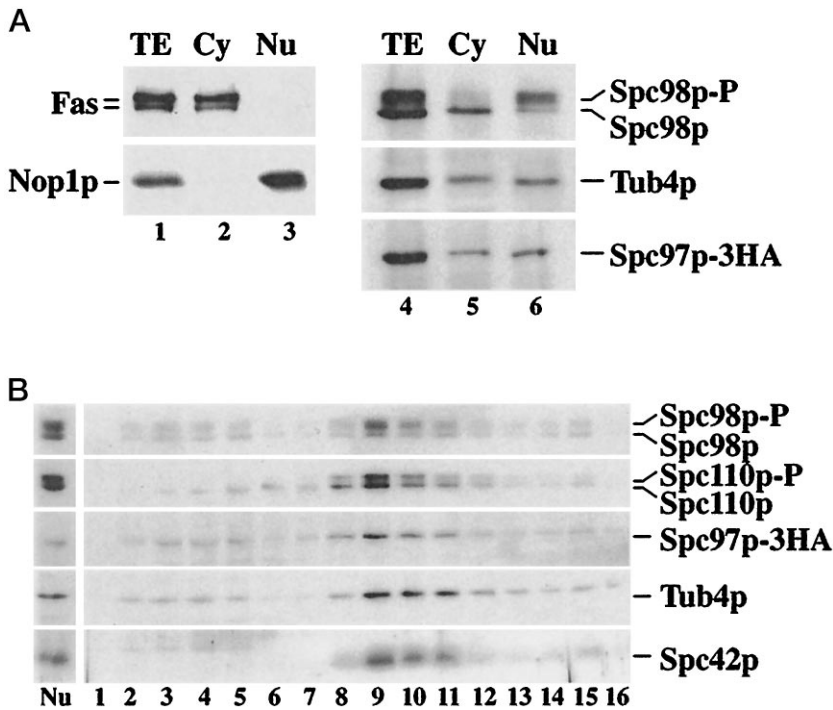
Figure 9. Spc98p phosphorylation is dependent on its cellular localization. (A) Lysed spheroblasts (TE) (lanes 1 and 4) were separated into cytoplasmic (Cy) (lanes 2 and 5) and nuclear fractions (Nu) (lanes 3 and 6) (see MATERIALS AND METHODS). The success of this fractionation (lanes 1–3) was established by following the cytoplasmic marker fatty acid synthase (Fas) and the nuclear marker nucleolin (Nop1p). Shown are immunoblots developed with anti-Fas or anti-Nop1p antibodies. Nuclei were solubilized with detergent in the presence of deoxyribonuclease I. Spc98p in the cytoplasmic and nuclear fractions was precipitated with anti-Spc98p antibodies. Tub4p, Spc98p, and Spc97p-3HA were detected in the immunoprecipitated material by immunoblotting using polyclonal antibodies. (B) Spc98p at the SPB is mainly phosphorylated. SPBs from wild-type cells were isolated by sucrose density centrifugation as described by Rout and Kilmartin (1990) in the presence of phosphatase inhibitors. The step gradient from 1.0 M (lane 1) to 2.5 M sucrose (lane 16) was fractionated. The lysed nuclei (Nu) (material that was layered on top of the sucrose gradient) and equal volumes of the gradient fractions (lanes 1–16) were analyzed by SDS-PAGE and immunoblotting for Spc98p, Spc110p, Spc97p-3HA, Tub4p, and Spc42p. SPBs were present in fractions 8–12, corresponding to approximately 2.0 M sucrose.

ever, the ratio of phosphorylated to unphosphorylated Spc98p increases from isolated nuclei to SPBs by a factor of 1.5 to 2, which is consistent with the view that Spc98p in the nucleoplasm is predominantly unphosphorylated. Again, this argues against a role of Spc98p phosphorylation in triggering nuclear import.

Interaction between two of the three components of the Tub4p complex was observed after co-overexpression (Figure 8A). These interactions correlated with data from two-hybrid experiments and suggest mutual interactions among Spc98p, Spc97p, and Tub4p (Geissler et al., 1996; Knop et al., 1997). In addition, Tub4p and Spc97p probably bind to different domains of Spc98p. This model is supported by the finding that a central domain of Spc98p (amino acids 147–551) exists that interacts specifically with Spc97p, while the carboxy-terminal portion (amino acids 511–846) binds only to Tub4p (Figure 8B). Previously, we have shown that the Spc98p derivative containing amino acids 390–846 does not interact with Tub4p in the two-hybrid system (Geissler et al., 1996). This discrepancy may be explained by the misfolding or aggregation of the truncated Gal4p-Spc98p[390–846] protein. Similar observations have been reported for other proteins (Geiser et al., 1993).

Phosphorylation of Spc98p

Cell-cycle dependent phosphorylation of centrosomal proteins in mammalian, *Schizosaccharomyces pombe*,

and *Aspergillus nidulans* cells has been detected using the monoclonal antibody MPM-2 (Vandre et al., 1984; Engle et al., 1988; Masuda et al., 1992), which is directed against mitosis-specific phosphoepitopes (Davis et al., 1983). This antibody does not stain the *S. cerevisiae* SPB (Schiebel, unpublished results), leaving it at first unclear whether *S. cerevisiae* SPB components are modified by phosphorylation. Spc42p and Spc110p are the first SPB components for which phosphorylation has been demonstrated (Donaldson and Kilmartin, 1996; Friedmann et al., 1996). Spc110p is a filamentous protein that connects the central with the inner plaque (Rout and Kilmartin, 1990; Kilmartin et al., 1993). Its amino-terminal domain interacts with Spc98p and Spc97p of the Tub4p complex (Knop and Schiebel, 1997). Spc42p forms a two-dimensional crystal within the SPB (Donaldson and Kilmartin, 1996; Bullitt et al., 1997). It has been isolated upon high-salt fragmentation of SPBs in complex with Spc110p, calmodulin, and an essential SPB component with an apparent molecular weight of 35 kDa (Knop and Schiebel, 1997; Schiebel, unpublished results).

Here we identified Spc98p as the first protein in a γ-tubulin complex that is subject to phosphorylation (Figure 1). The existence of homologs to Spc98p in the human, *X. laevis*, and *Drosophila* γ-tubulin complexes (Murphy and Stearns, personal communication; Zheng, personal communication) make this finding especially important. It is interesting to note that the
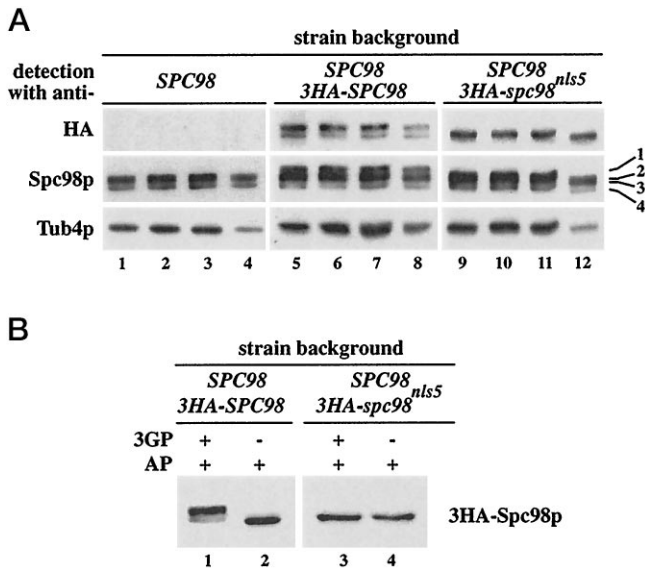
A

strain background

detection with anti-

| | SPC98 | SPC98 3HA-SPC98 | SPC98 3HA-spc98^{nls5} |

HA

Spc98p

Tub4p

1 2 3 4   5 6 7 8   9 10 11 12

B

strain background

	SPC98 3HA-SPC98		SPC98 3HA-spc98^{nls5}	
3GP	+	-	+	-
AP	+	+	+	+

3HA-Spc98p

1   2   3   4

Figure 10. Spc98p at the outer plaque of the SPB is not phosphorylated. (A) SPBs of cells expressing *SPC98* (lanes 1–4), *SPC98* and *3HA-SPC98* (lanes 5–8), or *SPC98* and *3HA-spc98*^{nls5} (lanes 9–12) were isolated by sucrose density gradient centrifugation. The gradients were fractionated, and the four fractions containing SPBs (fractions 8–11 of the sucrose gradient; see also Figure 9B) were analyzed by immunoblotting using anti-HA, anti-Spc98p, and anti-Tub4p antibodies. The numbers on the right indicate the phosphorylated (1) and nonphosphorylated (3) forms of 3HA-Spc98p, and the phosphorylated (2) and nonphosphorylated (4) forms of Spc98p, detected by the anti-Spc98p antibodies. Note that band 1 is not present in lanes 9–12. (B) 3HA-Spc98p^{nls5} is not phosphorylated. SPBs from cells expressing *SPC98* and *3HA-SPC98* (lanes 1 and 2) or *SPC98* and *3HA-spc98*^{nls5} (lanes 3 and 4) were solubilized with detergent. Detergent extracts were incubated with AP in the presence (lanes 1 and 3) or absence (lanes 2 and 4) of the inhibitor 3-glycerophosphate (3GP) (100 mM). Samples were analyzed by immunoblotting with anti-HA antibodies.

Drosophila homolog of Spc98p, p109, appears as a doublet (Zheng *et al.*, 1995; Zheng, personal communication), raising the possibility that this protein is also phosphorylated. Our analysis revealed that Spc98p is probably phosphorylated at multiple sites, as it is resolved in at least three bands by SDS-PAGE, which are all converted by either AP or serine/threonine-specific phosphatase PP2A to the fastest migrating, unphosphorylated form (Figure 1, B and C). Similar to Spc110p (Friedmann *et al.*, 1996; Stirling and Stark, 1996) and Spc42p (Donaldson and Kilmartin, 1996), Spc98p is subject to cell cycle-dependent phosphorylation. Spc98p becomes phosphorylated after SPB duplication, a conclusion that is supported by the *cdc4* experiment (Figure 4). Phosphorylation occurs during DNA replication (Figure 2, A and B), but clearly before Spc110p phosphorylation (Friedmann *et al.*, 1996). It will be interesting to determine whether Spc110p phosphorylation depends on the previous modification of Spc98p. This is a possibility, since Spc98p in-
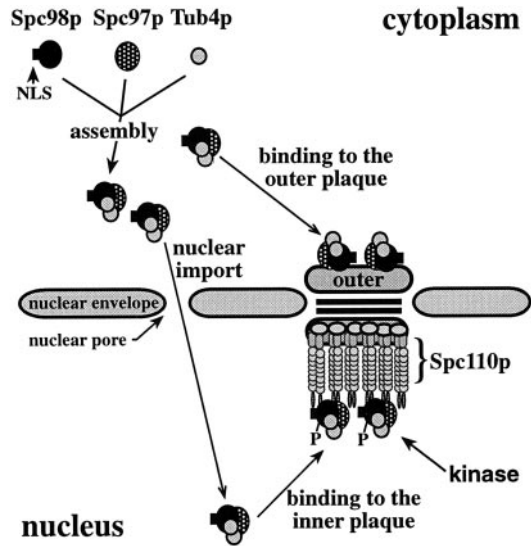

Figure 11. Model for formation, nuclear transport, and phosphorylation of the Tub4p complex. Substructures of the SPB were drawn as described (Bullitt *et al.*, 1997; Knop and Schiebel, 1997).

teracts with the amino-terminal domain of Spc110p at the SPB (Knop and Schiebel, 1997). Furthermore, our data are consistent with the notion that Spc98p at the inner plaque of the SPB is mainly phosphorylated, while at the outer plaque it is not: isolated SPBs contain phosphorylated as well as nonphosphorylated Spc98p (Figure 9B), and a nuclear import-deficient version of Spc98p, Spc98p^{nls5}, localized at the outer plaque (Figure 6D) in a predominantly unphosphorylated state (Figure 10).

Spc98p phosphorylation was affected in the temperature-sensitive kinase mutants *cdc7–1*, *cdc28*, and *mps1–1* (Figure 3A). The *cdc28* cells arrest at start of the cell cycle at which point Spc98p phosphorylation is minimal. *cdc7–1* cells arrests at late G1/S-phase, before the initiation of DNA synthesis (Byers and Goetsch, 1974; Hartwell, 1976; Yoon and Campbell, 1991). This arrest point coincides with the time Spc98p phosphorylation begins, explaining why Spc98p is predominantly phosphorylated in *cdc7–1* cells. *mps1–1* was found in a phenotypic screen for mutants that affect spindle formation (Winey *et al.*, 1991). *MPS1* encodes an essential protein kinase with functions in SPB duplication and mitotic checkpoint control (Winey *et al.*, 1991; Lauzé *et al.*, 1995; Hardwick *et al.*, 1996; Weiss and Winey, 1996). The localization of Mps1p has not been determined; however, it accumulates inside the nucleus when overproduced (Weiss and Winey, personal communication). Mps1p is active after start of the cell cycle and is induced by treatment of cells with hydroxyurea or nocodazole (Steiner and Winey, personal communication). These properties of Mps1p correlate well with the phosphorylation of Spc98p, rais-

ing the possibility that Mps1p kinase phosphorylates Spc98p.

What is the function of Spc98p phosphorylation? The nonphosphorylation of Spc98p in *cdc4–1* cells (Figure 4), excludes a role in SPB duplication or microtubule nucleation by the newly formed SPB. Furthermore, dephosphorylation of the isolated Tub4p complex by AP does not influence its composition or stability with respect to binding of Tub4p and Spc97p (Pereira, unpublished). Phosphorylation of Spc98p may influence microtubule attachment to the inner plaque of the SPB after the nucleation step. This may be essential to allow microtubule fluxes in mitosis (Mitchison, 1989; Sawin and Mitchison, 1994). Alternatively, reorganization of the Tub4p complex may be required to balance forces on the inner plaque of the SPB caused by chromosome and spindle movements in metaphase and anaphase (reviewed by McIntosh and Koonce, 1989). In this context it is interesting to note that *tub4–1* cells nucleate microtubules and form a short bipolar spindle as wild-type cells. The *tub4–1* spindle than collapses at the time the cells enter mitosis (Spang *et al.*, 1996a). Our results also suggest that the Tub4p complex at the outer and inner plaques is differently regulated, which may reflect the distinct roles of the cytoplasmic and nuclear microtubules (Huffaker *et al.*, 1987; Sullivan and Huffaker, 1992). Finally, Spc98p phosphorylation in response to mitotic checkpoint activation (Figure 3, C and D) may assist accurate chromosome segregation after disturbing the mitotic spindle. Due to these characteristics, phosphorylation of Spc98p proteins in γ-tubulin complexes may prove to be an important determinant for microtubule organization as well as a target that is modified in response to checkpoint activation.

ACKNOWLEDGMENTS

REFERENCES

Akashi, T., Yoon, Y., and Oakley, B.R. (1997). Characterization of γ-tubulin complexes in *Aspergillus nidulans* and detection of putative γ-tubulin interacting proteins. Cell Motil. Cytoskeleton *37*, 149–158.

Bradford, M.M. (1976). A rapid and sensitive method for the quantitation of microgram quantities of protein utilizing the principle of protein-dye binding. Anal. Biochem. *72*, 248–254.

Bullitt, E., Rout, M.P., Kilmartin, J.V., and Akey, C.W. (1997). The yeast spindle pole body is assembled around a central crystal of Spc42p. Cell *89*, 1077–1086.

Byers, B. (1981). Cytology of the yeast life cycle. In: The Molecular Biology of the Yeast *Saccharomyces*, ed. J.N. Strathern, E.W. Jones,

and J.R. Broach, Cold Spring Harbor, NY: Cold Spring Harbor Laboratory Press, 59–96.

Byers, B., and Goetsch, L. (1974). Duplication of spindle plaques and integration of the yeast cell cycle. Cold Spring Harbor Symp. Quant. Biol. *38*, 123–131.

Byers, B., and Goetsch, L. (1975). Behaviour of spindles and spindle plaques in the cell cycle and conjugation of *Saccharomyces cerevisiae*. J. Bacteriol. *124*, 511–523.

Christianson, T.W., Sikorski, R.S., Dante, M., Shero, J.H., and Hieter, P. (1992). Multifunctional yeast high-copy-number shuttle vectors. Gene *110*, 119–122.

Davis, F.M., Tsao, T.Y., Fowler, S.K., and Rao, P.N. (1983). Monoclonal antibodies to mitotic cells. Proc. Natl. Acad. Sci. USA *80*, 2926–2930.

Dingwall, C., and Laskey, R.A. (1991). Nuclear targeting sequences - a consensus? Trends Biochem. Sci. *16*, 478–481.

Donaldson, A.D., and Kilmartin, J.V. (1996). Spc42p: A phosphorylated component of the *S. cerevisiae* spindle pole body (SPB) with an essential function during SPB duplication. J. Cell Biol. *132*, 887–901.

Durfee, T., Becherer, K., Chen, P.-L., Yeh, S.-H., Yang, Y., Kilburn, A.E., Lee, W.-H., and Elledge, S.J. (1993). The retinoblastoma protein associates with the protein phosphotase type 1 catalytic subunit. Genes Dev. *7*, 555–569.

Engle, D.B., Doonan, J.H., and Morris, N.R. (1988). Cell cycle modulation of MPM-2 specific spindle pole body phosphorylation in *Aspergillus nidulans*. Cell Motil. Cytoskeleton *10*, 432–437.

Friedmann, D.B., Sundberg, H.A., Huang, E.Y., and Davis, T.N. (1996). The 110-kD spindle pole body component of *Saccharomyces cerevisiae* is a phosphoprotein that is modified in a cell cycle-dependent manner. J. Cell Biol. *132*, 903–914.

Geiser, J.R., Sundberg, H.A., Chang, B.H., Muller, E.G.D., and Davis, T.N. (1993). The essential mitotic target of calmodulin is the 110-kilodalton component of the spindle pole body in *Saccharomyces cerevisiae*. Mol. Cell. Biol. *13*, 7913–7924.

Geissler, S., Pereira, G., Spang, A., Knop, M., Souès, S., Kilmartin, J., and Schiebel, E. (1996). The spindle pole body component Spc98p interacts with the γ-tubulin-like Tub4p of *Saccharomyces cerevisiae* at the sites of microtubule attachment. EMBO J. *15*, 3899–3911.

Graham, T.R., and Emr, S.D. (1991). Compartmental organization of Golgi-specific protein modification and vacuolar sorting events defined in yeast *sec18* (NSF) mutant. J. Cell Biol. *114*, 207–218.

Gyuris, J., Golemis, E., Chertkov, H., and Brent, R. (1993). Cdi1, a human G1 and S phase protein phosphatase that associates with Cdk2. Cell *75*, 791–803.

Hardwick, K.G., Weiss, E., Luca, F.C., Winey, M., and Murray, A.W. (1996). Activation of the budding yeast spindle assembly checkpoint without mitotic spindle disruption. Science *273*, 953–956.

Harlow, E., and Lane, D. (1988). Antibodies: A Laboratory Manual. Cold Spring Harbor, NY: Cold Spring Harbor Laboratory Press.

Hartwell, L.H. (1976). Sequential function of gene products relative to DNA synthesis in the yeast cell cycle. J. Mol. Biol. *104*, 803–817.

Hartwell, L.H., and Weinert, T.A. (1989). Checkpoints: controls that ensure the order of cell cycle events. Science *246*, 629–634.

Henkel, T., Zabel, U., Zee, K.v., Müller, J.M., Fanning, E., and Baeuerle, P.A. (1992). Intramolecular masking of the nuclear location signal and dimerization domain in the precursor for the p50 NF-κB subunit. Cell *68*, 1121–1133.

Horio, T., Uzawa, S., Jung, M.K., Oakley, B.R., Tanaka, K., and Yanagida, M. (1991). The fission yeast γ-tubulin is essential for mitosis and is localized at microtubule organizing centers. J. Cell Sci. *99*, 693–700.

Hoyt, M.A., Totis, L., and Roberts, B.T. (1991). *S. cerevisiae* genes required for cell-cycle arrest in response to loss of microtubule function. Cell *66*, 507–517.

Huffaker, T.C., Hoyt, M.A., and Botstein, D. (1987). Genetic analysis of the yeast cytoskeleton. Annu. Rev. Genet. *21*, 259–284.

Hutter, K.J., and Eipel, H.E. (1979). Microbial determination by flow cytometry. J. Gen. Microbiol. *113*, 369–375.

Kellogg, D.R., Moritz, M., and Alberts, B.M. (1994). The centrosome and cellular-organization. Annu. Rev. Biochem. *63*, 639–674.

Kilmartin, J.V., Dyos, S.L., Kershaw, D., and Finch, J.T. (1993). A spacer protein in the *Saccharomyces cerevisiae* spindle pole body whose transcription is cell-cycle regulated. J. Cell Biol. *123*, 1175–1184.

Kilmartin, J.V., and Goh, P.-Y. (1996). Spc110p: Assembly properties and role in the connection of nuclear microtubules to the yeast spindle pole body. EMBO J. *15*, 4592–4602.

Knop, M., Finger, A., Braun, T., Hellmuth, K., and Wolf, D.H. (1996). Der1, a novel protein specifically required for endoplasmic reticulum degradation in yeast. EMBO J. *15*, 753–763.

Knop, M., Pereira, G., Geissler, S., Grein, K., and Schiebel, E. (1997). The spindle pole body component Spc97p interacts with the γ-tubulin of *Saccharomyces cerevisiae* and functions in microtubule organization and spindle pole body duplication. EMBO J. *16*, 1550–1564.

Knop, M., and Schiebel, E. (1997). Spc98p and Spc97p of the yeast γ-tubulin complex mediate binding to the spindle pole body via their interaction with Spc110p. EMBO J. *16*, 6985–6995.

Laemmli, U.K. (1970). Cleavage of structural proteins during the assembly of the head of bacteriophage T4. Nature *227*, 680–685.

Lauzé, E., Stoelcker, B., Luca, F.C., Weiss, E., Schutz, A.R., and Winey, M. (1995). Yeast spindle pole body duplication gene *MPS1* encodes an essential dual specificity protein kinase. EMBO J. *14*, 1655–1663.

Li, R., and Murray, A.W. (1991). Feedback control of mitosis in budding yeast. Cell *66*, 519–531.

Lopez, I., Khan, S., Sevik, M., Cande, W.Z., and Hussey, P.J. (1995). Isolation of a full-length cDNA encoding *Zea mays* γ-tubulin. Plant Physiol. *107*, 309–310.

Mandelkow, E.-M., and Mandelkow, E. (1993). α/β-Tubulin. In: Guidebook to the Cytoskeletal and Motor Proteins, ed. T. Kreis and R. Vale, Oxford, UK: Oxford University Press, 127–130.

Marschall, L.G., Jeng, R.L., Mulholland, J., and Stearns, T. (1996). Analysis of Tub4p, a yeast γ-tubulin-like protein: implications for microtubule-organizing center function. J. Cell Biol. *134*, 443–454.

Masuda, H., Sevik, M., and Cande, W.Z. (1992). In vitro microtubule-nucleating activity of spindle pole bodies in fission yeast *Schizosaccharomyces pombe*: cell cycle-dependent activation in *Xenopus* cell-free extracts. J. Cell Biol. *117*, 1055–1066.

McIntosh, J.R., and Koonce, M.P. (1989). Mitosis. Science *246*, 622–628.

Mitchell, D.A., Marshall, T.K., and Deschenes, R.J. (1993). Vectors for the inducible overexpression of glutathione S-transferase fusion proteins in yeast. Yeast *9*, 715–723.

Mitchison, T.J. (1989). Polewards microtubule flux in the mitotic spindle: Evidence from photoactivation of fluorescence. J. Cell Biol. *109*, 637–652.

Moll, T., Tebb, G., Surana, U., Robitsch, H., and Nasmyth, K. (1991). The role of phosphorylation and the CDC28 protein kinase in cell cycle-regulated nuclear import of the *S. cerevisiae* transcription factor SWI5. Cell *66*, 743–758.

Moritz, M., Braunfeld, M.B., Fung, J.C., Sedat, J.W., Alberts, B.M., and Agard, D.A. (1995a). Three-dimensional structural characterization of centrosomes from early *Drosophila* embryos. J. Cell Biol. *130*, 1149–1159.

Moritz, M., Braunfeld, M.B., Sedat, John W., Alberts, B., and Agard, D.A. (1995b). Microtubule nucleation by γ-tubulin-containing rings in the centrosome. Nature *378*, 638–640.

Moudjou, M., Bordes, N., Paintrand, M., and Bornens, M. (1996). γ-tubulin in mammalian cells: The centrosomal and the cytosolic forms. J. Cell Sci. *109*, 875–887.

Murray, A.W. (1992). Creative blocks: cell-cycle checkpoints and feedback controls. Nature *359*, 599–604.

Myers, A.M., Tzagoloff, A., Kinney, D.M., and Lusty, C.J. (1986). Yeast shuttle and integrative vectors with multiple cloning sites suitable for construction of *lacZ* fusion. Gene *45*, 299–310.

Nasmyth, K. (1993). Control of the yeast cell cycle by the Cdc28p protein kinase. Curr. Opin. Cell Biol. *5*, 166–179.

Oakley, B.R. (1992). γ-tubulin: The microtubule organizer? Trends Cell Biol. *2*, 1–5.

Oakley, B.R., Oakley, E., Yoon, Y., and Jung, M.K. (1990). γ-Tubulin is a component of the spindle pole body that is essential for microtubule function in *Aspergillus nidulans*. Cell *61*, 1289–1301.

Oakley, C.E., and Oakley, B.R. (1989). Identification of γ-tubulin, a new member of the tubulin superfamily encoded by *mipA* gene of *Aspergillus nidulans*. Nature *338*, 662–664.

Pereira, G., and Schiebel, E. (1997). Centrosome-microtubule nucleation. J. Cell Sci. *110*, 295–300.

Pickett-Heaps, J.D. (1969). The evolution of the mitotic apparatus: An attempt at comparative ultrastructural cytology in dividing plant cells. Cytobios *3*, 257–280.

Reneke, J.E., Blumer, K.J., Courchesne, W.E., and Thorner, J. (1988). The carboxy-terminal segment of the yeast α-factor receptor is a regulatory domain. Cell *55*, 221–234.

Rout, M.P., and Kilmartin, J.V. (1990). Components of the yeast spindle and spindle pole body. J. Cell Biol. *111*, 1913–1927.

Rubin, G.M. (1973). The nucleotide sequence of *Saccharomyces cerevisiae* 5.8S ribosomal ribonucleic acid. J. Biol. Chem. *248*, 3860–3875.

Sanger, F., Nicklen, S., and Coulson, A.R. (1977). DNA sequencing with chain-terminating inhibitors. Proc. Natl. Acad. Sci. USA *74*, 5463–5467.

Sawin, K.E., and Mitchison, T.J. (1994). Microtubule flux in mitosis is independent of chromosomes, centrosomes, and antiparallel microtubules. Mol. Biol. Cell *5*, 217–226.

Schiestl, R.H., and Gietz, R.D. (1989). High efficiency transformation of intact yeast cells using stranded nucleic acids as a carrier. Curr. Genet. *16*, 339–346.

Schweitzer, B.I., and Philippsen, P. (1991). *CDC15*, an essential cell cycle gene in *Saccharomyces cerevisiae*, encodes a protein kinase domain. Yeast *7*, 265–273.

Sherman, F. (1991). Getting started with yeast. Methods Enzymol. *194*, 3–21.

Sikorski, R.S., and Hieter, P. (1989). A system of shuttle vectors and yeast host strains designed for efficient manipulation of DNA in *Saccharomyces cerevisiae*. Genetics *122*, 19–27.

Sobel, S.G., and Snyder, M. (1995). A highly divergent γ-tubulin gene is essential for cell growth and proper microtubule organization in *Saccharomyces cerevisiae*. J. Cell Biol. *131*, 1775–1788.

Spang, A., Geissler, S., Grein, K., and Schiebel, E. (1996a). γ-tubulin-like Tub4p of *Saccharomyces cerevisiae* is associated with the spindle pole body substructures that organize microtubules and is required for mitotic spindle formation. J. Cell Biol. *134*, 429–441.

Spang, A., Grein, K., and Schiebel, E. (1996b). The spacer protein Spc110p targets calmodulin to the central plaque of the yeast spindle pole body. J. Cell Sci. *119*, 2229–2237.

Stearns, T., Evans, L., and Kirschner, M. (1991). γ-tubulin is a highly conserved component of the centrosome. Cell *65*, 825–836.

Stearns, T., and Kirschner, M. (1994). In vitro reconstitution of centrosome assembly and function: The central role of γ-tubulin. Cell *76*, 623–637.

Stirling, D.A., and Stark, M.J. (1996). The phosphorylation state of the 110 kDa component of the yeast spindle pole body shows cell cycle dependent regulation. Biochem. Biophys. Res. Commun. *222*, 236–242.

Sullivan, D.S., and Huffaker, T.C. (1992). Astral microtubules are not required for anaphase B in *Saccharomyces cerevisiae*. J. Cell Biol. *119*, 379–388.

Vandre, D.D., Davis, F.M., Rao, P.N., and Borisy, G.G. (1984). Phosphoproteins are components of mitotic microtubule organizing centres. Proc. Natl. Acad. Sci. USA *81*, 4439–4443.

Weil, C.F., Oakley, C.E., and Oakley, B.R. (1986). Isolation of *mip* (microtubule-interacting protein) mutations of *Aspergillus nidulans*. Mol. Cell. Biol. *6*, 2963–2968.

Weiss, E., and Winey, M. (1996). The *Saccharomyces cerevisiae* spindle pole body duplication gene *MPS1* is part of a mitotic check point. J. Cell Biol. *132*, 111–123.

Winey, M., Goetsch, L., Baum, P., and Byers, B. (1991). *MPS1* and *MPS2*: Novel yeast genes defining distinct steps of spindle pole body duplication. J. Cell Biol. *114*, 745–754.

Yoon, H.-J., and Campbell, J.L. (1991). The CDC7 protein of *Saccharomyces cerevisiae* is a phosphoprotein that contains protein kinase activity. Proc. Natl. Acad. Sci. USA *88*, 3574–3578.

Young, M.R., and Tyk, B.K. (1997). Mcm2 and Mcm3 are constitutive nuclear proteins that exhibit distinct isoforms and bind chromatin during specific cell cycle stages of *Saccharomyces cerevisiae*. Mol. Biol. Cell *8*, 1587–1601.

Zheng, Y., Jung, K., and Oakley, B.R. (1991). γ-tubulin is present in *Drosophila melanogaster* and *Homo sapiens* and is associated with the centrosome. Cell *65*, 817–823.

Zheng, Y., Wong, M.L., Alberts, B., and Mitchison, T. (1995). Nucleation of microtubule assembly by a γ-tubulin-containing ring complex. Nature *378*, 578–583.